Review article: Performance assessment of radiation-based field sensors for monitoring the water equivalent of snow cover (SWE)

Alain Royer[a,b*], Alexandre Roy[b,c], Sylvain Jutras[d], Alexandre Langlois[a,b]

[a]Centre d'Applications et de Recherche en Télédétection (CARTEL), Université de Sherbrooke, Sherbrooke, Québec, Canada
[b]Centre d'études nordiques (CEN), Québec, Canada
[c]Département des Sciences de l'Environnement, Université du Québec à Trois-Rivières, Trois-Rivières, Québec, Canada
[d]Département des sciences du bois et de la forêt, Université Laval, Québec City, Québec, Canada
* Corresponding author

Abstract

Continuous and spatially distributed data of snow mass (water equivalent of snow cover, SWE) from automatic ground-based measurements are increasingly required for climate change studies and for hydrological applications (snow hydrological model improvement and data assimilation). We present and compare four new-generation sensors, now commercialized, that are non-invasive based on different radiations that interact with snow for SWE monitoring: Cosmic Ray Neutron Probe (CRNP); Gamma Ray Monitoring (GMON) scintillator; frequency-modulated continuous-wave radar (FMCW-Radar) at 24 GHz; and Global Navigation Satellite System (GNSS) receivers (GNSSr). All four techniques have relatively low power requirements, provide continuous and autonomous SWE measurements, and can be easily installed in remote areas. A performance assessment of their advantages, drawbacks and uncertainties are discussed from experimental comparisons and a literature review. Relative uncertainties are estimated to range between 9 and 15% when compared to manual in situ snow surveys that are also discussed. Results show: • CRNP can be operated in two modes of functioning: beneath the snow, it is the only system able to measure very deep snowpacks (> 2000 mm w.e.) with reasonable uncertainty across a wide range of measurements; CRNP placed above the snow allows SWE measurements over a large footprint (∼20 ha) above a shallow snowpack; in both cases, CRNP needs ancillary atmospheric measurements for SWE retrieval. • GMON is the most mature instrument for snowpacks that are typically up to 800 mm w.e.; Both instruments, CRNP (above snow) and GMON, are sensitive to surface soil moisture. • FMCW-Radar needs auxiliary snow depth measurements for SWE retrieval and is not recommended for automatic SWE monitoring (limited to dry snow). FMCW-radar is very sensitive to wet snow, making it a very useful sensor for melt detection (e.g., wet avalanche forecasts); • GNSSr allows three key snowpack parameters to be estimated simultaneously: SWE (range: 0 - 1000 mm w.e.), snow depth and liquid water content, according to the retrieval algorithm that is used. Its low cost, compactness and low mass suggest a strong potential for GNSSr application in remote areas.

Key word: Water equivalent of snow cover, electromagnetic wave sensors, Cosmic Ray Neutron Probe, Gamma Ray Monitoring, frequency-modulated continuous-wave radar, Global Navigation Satellite System, sensor performance review

1. Introduction

Snow cover on the ground surface plays an important role in the climate system due to its high albedo, heat insulation that affects the ground thermal regime, and its contribution to snow runoff and soil moisture. Water equivalent of snow cover (noted SWE, its mass per unit area) is expressed in kg m^{-2}, but also is commonly shown in units of mm of water equivalent, mm w.e. It is an Essential Climate Variable (ECV) for monitoring climate change, as recognized by the Global Climate Observing System (GCOS-WMO, 2016; https://gcos.wmo.int/en/essential-climate-variables.), which aligns with the WMO-Global Cryosphere Watch Initiative (Key et al., 2016; https://globalcryospherewatch.org). SWE monitoring is also of primary importance for hydrological forecasting and preventing flooding risks over snowmelt-dominated basins in mountainous and cold climate regions. Snow station distributions are generally sparse in high latitude regions, remote areas and high mountains (Bormann et al., 2013; Key et al., 2015, 2016; Pirazzini et al., 2018; Haberkorn, 2019; Brown et al., 2019, 2021; Royer et al., 2021), given that monitoring is generally based upon expensive and occasional (weekly to monthly) manual sampling. Automation of SWE measurement networks is an essential medium-term prospect, especially since reliable and automatic instrument alternatives exist (Dong, 2018; this study).

Various in situ field devices and approaches for measuring the temporal dynamics of SWE are available, all of which have their strengths and limitations (see the review by Rasmussen et al., 2012; Kinar and Pomeroy, 2015; Pirazzini et al., 2018). Some are invasive (i.e., destroying the snowpack or changing its properties), while others that are based on different remotely sensed approaches are non-invasive. Here, we focus on a new generation of radiation-based field sensors that directly measure SWE, i.e., measuring a signal that is proportional to the snow mass per unit area. In this study, we do not consider sensors that are based on pressure and load cell sensors (snow pillows), snowmelt lysimeters, dielectric sensors (e.g., the SNOWPOWER system, commercially available as the Snowpack Analyzer) or acoustic sensors (see Kinar and Pomeroy, 2015). Neither do we consider indirect approaches, such as those based on snow-depth monitoring, combined with a model of snow density evolution (Yao et al., 2018). We also exclude satellite-based approaches.

The objective of this paper, therefore, is to present a performance review of four selected non-invasive sensors (Table 1), viz., the Cosmic Ray Neutron Probe (CRNP), the Gamma Ray Monitoring (GMON) scintillator, frequency-modulated continuous-wave radar (FMCW-Radar) and Global Navigation Satellite System (GNSS) receivers (GNSSr). All four approaches have common features: easy to install; low power (e.g., powered by solar panels); provide continuous and autonomous SWE measurements; and deployable in remote areas. The continuous or quasi-continuous SWE measurement capability is

89 defined here relative to the application, such as for seasonal SWE monitoring, for
90 hydrological model validation, or to follow an event of a relatively short winter storm.
91 Surface-based radar scatterometers and microwave radiometers have not been
92 considered in this study because 1) they are still in early stages of development or are
93 currently not operational, and 2) they have heavy maintenance demands (not
94 autonomous) and are still relatively expensive. These include, for example,
95 scatterometers (Werner et al., 2010; Wiesmann et al., 2010; King et al., 2015; Werner et
96 al., 2019), microwave radiometers (Langlois, 2015; Roy et al., 2016, 2017; Wiesmann et
97 al., 2021); radar interferometers (Werner et al., 2010; Leinss et al., 2015; Pieraccini and
98 Miccinesi, 2019; GPRI brochure, 2021), and Stepped-Frequency Continuous Wave Radar
99 (SFCW) instruments (Alonso et al., 2021).
100
101 Sect. 2 provides background information on the basic principles of each of the four
102 sensors that are presented in Table 1. Examples of SWE temporal series comparisons from
103 four different instruments that were acquired in Québec, Eastern Canada, are given in
104 Sect. 3.1 and 3.2: comparisons between EDF's CRNP (NRC sensor) and GMON on one
105 hand, and GNSSr, FMCW-Radar and GMON on the other hand. This permits performance
106 evaluations for each system, including uncertainty analysis, compared to manual SWE
107 measurements. We complement these uncertainty assessments with a review of
108 additional results from previous studies (Sect. 3.3, Table 2). Advantages and drawbacks
109 of these sensors are then discussed in Sect. 4 (Table 3).
110
111 **2.** Radiation-based SWE sensor review
112 The main characteristics of the four reviewed sensors are summarized in Table 1, with the
113 acronym that is used to denote them, together with their commercial names. There are
114 two operation modes for the Cosmic Ray Neutron Probe (CRNP); thus, five cases were
115 considered. All of these sensors allow quasi-continuous measurements throughout the
116 winter without maintenance, and are powered by solar panels and batteries. The
117 measuring principles of each of the instruments are illustrated in Fig. 1 and shown in Fig.
118 2. In this section, we only recall the main principles of functioning and the key elements
119 of SWE retrieval, given that all sensors are well described in detail in the cited references.
120
121 Aspects that are related to the measurement scale of each sensor are critical to SWE
122 measurements, since SWE is generally highly variable spatially, depending upon the
123 ecosystem and terrain (Kinar and Pomeroy, 2015; Dong, 2018). These questions are
124 discussed in Sect. 4.
125
126

127 *Table 1. SWE sensors that were studied and acronyms that were used. FMCW: frequency-*
128 *modulated continuous-wave radar; GNSS: Global Navigation Satellite System, including*
129 *GPS (USA), GLONASS (Russia), Galileo (Europe) and Beidou (China) satellite constellations.*
130 *The frequency (Freq.) of the electromagnetic (EM) wave that was used and their*
131 *approximate maximum Water equivalent of snow (SWE_{max}) measurement limit*
132 *capabilities are given. SD: snow depth. See Fig. 1 for measurement principle*
133 *conceptualization and Fig. 2 for photos.*

134

| Sensor	Acronym	Approach	Freq. GHz	SWE_{max} (mm w.e.)	Comments	Commercial Name	Main recent references
Cosmic Ray Neutron Probe	CRNP	Sensor beneath snowpack	-	up to 2000	Measures total snow, ice and water amount	SnowFox	https://hydroinnova.com
						Hydroinnova CRS-1000/B	https://hydroinnova.com Bogena et al., 2020
		Sensor above snowpack		~ 150-300		NRC EDF-Fr	Gottardi et al., 2013
						Cosmic Ray Detector (CRD)	Geonor Inc.
Gamma Ray scintillator	GMON	Sensor above snowpack	$3.53\ 10^{11}$ $6.31\ 10^{11}$	up to 600 - 800	Measures total snow, ice and water amount	CS725 Campbell Sci.	Choquette et al., 2013 Smith et al., 2017 http://www.campbellsci.ca
Frequency-modulated continuous-wave Radar	FMCW-Radar	Active sensor above snowpack	24	~1000	Requires SD measurements Also measures stratigraphy	Sentire™ sR-1200 IMST Inc.	Pomerleau et al., 2020 https://shop.imst.de
Global Navigation Satellite System receivers	GNSSr	2 antennas above/ beneath snowpack	1.575 - 1.609	Up to 1500	Measures also Liquid Water Content and estimates SD	SnowSense	Henkel et al., 2019 Koch et al., 2020 https://www.vista-geo.de/en/snowsense/

135
136
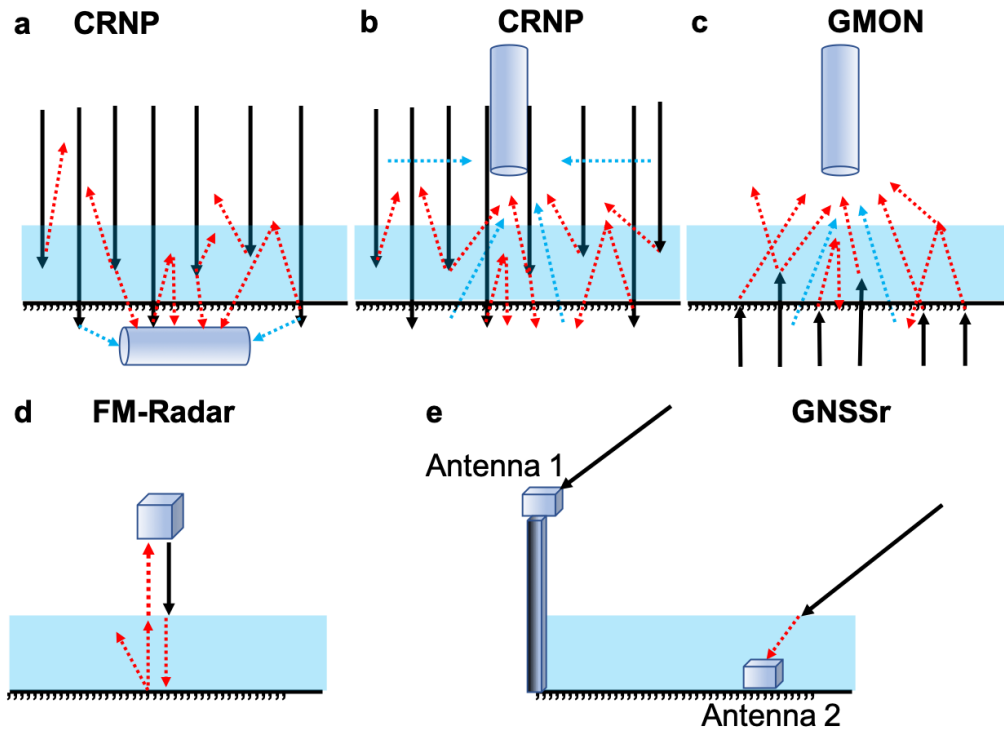
Figure 1 Diagram of radiation paths for the five approaches (see Table 1). In all figures, black arrows correspond to natural (a, b, c) or emitted (d, e) signals and dotted red arrows to rays interacting with snow (the lower the signal reaching the sensor, the higher the SWE). The "footprint" of the sensor is defined by the area from which emanates the measured radiation having interacted with the snow. **a)** Cosmic Ray Neutron Probe (CRNP) below the snow, buried in the ground. In this case, black arrows are ambient neutrons generated primarily by interactions of secondary cosmic ray neutrons with terrestrial and atmospheric nuclei. Dotted red arrows are neutrons interacting with snow, which decrease when SWE increases. Dotted blue arrows are neutrons interacting with soil moisture. **b)** CRNP above the snow, looking downward. Same as (a) for the arrow meanings, but dotted blue arrows are neutrons interacting with soil and atmospheric moisture. **c)** Gamma Ray Monitor (GMON) sensor. Same as (a) for the arrow meanings. **d)** Frequency-modulated continuous-wave radar (FMCW-Radar) looking downward above the snow. Black arrow is the radar-emitted wave at 24 GHz. **e)** Global Navigation Satellite System (GNSS) receivers. The two antennas receive signals emitted by all of the GNSS satellites in the antennas' field of view and at all incidence angles: only one incident ray (black arrow) at one angle is shown. According to the inversion algorithm, different rays that interact with the snow (dotted red arrows) are used. For the SnowSense system, independent measurements at antenna 1 and antenna 2 are analyzed.

Figure 2. Photographs of sensors that were analyzed. **a**) Cosmic Ray Neutron Probe (CRNP) from the EDF French network (Nivomètre à Rayon Cosmique, NRC) at the Lac noir station in Ecrins-Pelvoux massif, France. One can see the neutron probe buried in the ground (also shown in inset) and the mast, which carries ancillary meteorological sensors. Credit: Delunel et al. (2014). **b**) SnowFox CRNP set at ground level beneath the snow cover. Similar to (a), the system requires measurements of atmospheric conditions. Credit: Hydroinnova SnowFox manual. **c**) Same sensor as in (b)**,** but the Hydroinnova CRS-1000/B sensor is placed above the snow, measuring ambient and upward neutron counts, with the latter being attenuated by the snowpack. Crédit: Philip Marsh, Wilfrid Laurier University, Waterloo, ON, Canada; sensor in the tundra at Trail Valley Creek, Changing Cold Regions Network http://ccrnetwork.ca). **d**) GNSSr installed at the Université de Sherbrooke SIRENE site. The antenna that was placed on the ground (beneath the snow) was made visible at 3 m from the mast, on top of which a second antenna was affixed. Credits: Alain Royer. **e**) The FMCW-Radar (on the left) and the GMON (on the right) at the NEIGE-Forêt Montmorency site. A metallic plate on the ground in the field-of-view of the radar substantially increases radar echoes. In the background of photo (**e**), one can see the solid precipitation gauge, which is known as the Double Fence Intercomparison Reference (DFIR). Credits: Alain Royer. **f**) Meteorological and snow (GMON) automatic station at the LeMoyne James-Bay, Québec, Canada site in a sub-arctic environment (Prince et al., 2019). Credits: Alain Royer. **g**) The GMON at the NEIGE-Forêt Montmorency site set up to boost ^{40}K counts with pipes filled with potassium fertilizer. Credit: Sylvain Jutras.

2.1 Cosmic Ray Neutron probe (CRNP)

CRNP measurement is based on the moderation of ambient neutrons by hydrogen in water, snow and ice. The intensity of natural low-energy cosmic ray neutron emission is inversely correlated with the amount of hydrogen in the soil (Zreda et al. 2008; Andreasen et al., 2017) or snow cover (Desilets et al. 2010; Gottardi et al., 2013; Sigouin and Si, 2016; Gugerli et al., 2019; Bogena et al., 2020). Even though the principle of this approach has been known since the 1970s, it attained a level of operational maturity in the 2000s, especially with the use of commercialized soil moisture probes. Électricité de France (EDF)

6

182 successfully used a network of cosmic-ray probes (denoted Nivomètre à Rayon Cosmique,
183 NRC; this sensor is composed of two neutron detector tubes filled with Helium 3, ^{3}He)
184 that were buried under the snowpack to measure SWE for more than a decade in the
185 French Alps and in the Pyrenees (Fig. 2a, sensor placed at 3.5 m from a 6 m mast) (Paquet
186 and Laval, 2006; Paquet et al., 2008; Gottardi et al., 2013; Delunel et al., 2014).
187 Ephemeral, shallow snow cover across the UK is monitored by the COSMOS-UK network
188 of 46 sites equipped with the CRNP Hydroinnova CRS-2000 or CRS-1000/B models
189 (https://cosmos.ceh.ac.uk; Evans et al., 2016).
190
191 There are two experimental approaches for CRNP-based SWE monitoring (Fig. 1a,b): 1)
192 with the probe at the ground level beneath the snow (such as EDF' NRC, Fig. 2a, and the
193 SnowFox sensor for Hydroinnova, Fig. 2b), or 2) with the probe placed a few meters above
194 the snow surface (Fig. 1b), such as the one proposed by Hydroinnova (Fig. 2c) (CRS-
195 1000/B, Hydroinnova, Albuquerque, NM, USA; http://hydroinnova.com/
196 snow_water.html). Using dual-channel, the system is composed of two detector tubes
197 filled with ^{10}BF$_3$; one is sensitive to neutrons with a maximum energy of ~0.025 eV,
198 whereas the second is sensitive to moderated energy neutrons from ~0.2eV to 100 keV.
199 The cosmic ray probe above the snowpack (Fig. 1b) is an attractive SWE measurement
200 tool because it can provide direct estimates of SWE within a 20 to 40 ha measurement
201 area, 'footprint' (20 ha corresponds to a circle of 252 m radius) (Desilets and Zerda, 2013;
202 Schattan et al., 2017). In contrast, the footprint of a probe that is installed under the snow
203 is limited to a spot measurement above the sensor (Fig. 1a). While approach (1a) permits
204 measurements of very thick snow cover (> 1000 mm SWE) (Gugerli et al., 2019), the
205 drawback of approach (1b) is that it is limited to low SWE measurements (typically < 150
206 mm SWE) over homogeneous flat terrain. However, in the Austrian Alps, contrary to
207 previous studies, Schattan et al. (2017) claim not to have measured saturation for a
208 snowpack of the order of 600 mm SWE, over an estimated footprint with 230 m radius.
209
210 The CRNP method requires creating a function for converting neutron counts to SWE
211 (Paquet et al., 2008; Gottardi et al., 2013; Sigouin and Si, 2016; Andreasen et al., 2017;
212 Schattan et al., 2017; Delunel et al., 2014; Bogena et al., 2020). Desilets (2017) provides
213 the calibration procedure in detail. Neutron counts must be accumulated over a specified
214 period of time (e.g., from 6 h to 24 h). The CRNP method requires that the counting rate
215 must first be known (calibrated) and that disturbance effects on measured cosmic rays at
216 the site location have to be taken into account. Disturbance effects that need to be
217 corrected include temporal variations in the natural cosmic-ray flux and variations in air
218 pressure and atmospheric water vapor on site measurements during the count time.
219 Temporal variation in cosmic-ray flux can be determined from the NMDB database (Real-
220 Time Database for high-resolution Neutron Monitor measurements; www.nmdb.eu),
221 thereby providing access to reference neutron monitor measurements from stations
222 around the world. Corrections for air pressure (linked to the altitude of the station) and
223 atmospheric water vapor variations require ancillary standard meteorological sensors,
224 which measure atmospheric pressure, air temperature and relative humidity.
225

226 While accuracy losses that are linked to atmospheric disturbances (pressure and humidity
227 corrections) are relatively weak (a few percent), this is not the case for primary variations
228 in the natural cosmic-ray flux (Andreasen et al., 2017), which may drastically change the
229 results of SWE estimation. This flux can vary up to 30% over long periods (weeks to
230 months), thereby causing errors up to 50% in SWE estimates when they are not
231 considered (Paquet and Laval, 2006). Therefore, it is important to correct the measured
232 signal using the closest world reference station in the vicinity of the measurement site. If
233 not available, a second cosmic-ray sensor is required to produce accurate SWE estimates
234 using normalized signals (above and beneath snow) as done by the Cosmic Ray Detector
235 commercialized by Geonor Inc. (www.Geonor.com).
236
237 In the case of the second approach, where the probe is installed above the ground surface
238 (Fig. 1b), the probe must be calibrated for soil moisture. If soil moisture correction is not
239 applied on the winter signal measurements, retrieved SWE values will be systematically
240 overestimated. This bias can be corrected using measurements of CRNP signal without
241 snow, just prior to the onset of snow cover, or using soil moisture probe during the winter
242 (see Sect. 4).
243
244 2.2 Gamma Ray scintillator (GMON)
245 Monitoring SWE by using natural soil radioactivity is a well-known approach (Bissell and
246 Peck, 1973). Since 1980, an airborne snow survey program using this technology has
247 successfully collected areal mean SWE data for operational flood forecasting over the
248 whole of northwestern North America, including the Rocky Mountains, Alaska and Great
249 Plains (National Operational Hydrologic Remote Sensing Center,
250 https://www.nohrsc.noaa.gov/snowsurvey/). The mean areal SWE value is based on the
251 difference between gamma radiation measurements over bare ground and snow-covered
252 ground, the latter being attenuated by the snowpack (Carroll, 2001).
253
254 The principle of SWE measurements that are based on the Gamma Monitor (GMON) ray
255 scintillator is the absorption by the water, regardless of its phase (liquid, snow or ice), of
256 the natural radioactive emission of Potassium-40 (^{40}K) from soils (Ducharme et al., 2015).
257 This naturally occurring radioactive isotope of potassium has a gamma emission of 1.46
258 MeV. The GMON probe also measures the emission of Thallium-208 (^{208}Tl), which emits
259 gamma rays at a slightly higher energy (2.61 MeV) that originate from the decay of
260 Thorium 232 (Choquette et al., 2013; Wright, 2013; Stranden et al., 2015). Both of these
261 elements are common to almost all types of surfaces, regardless of whether these are
262 organic or non-organic soils. However, we observed that the isotope associated with the
263 higher count (i.e., ^{40}K) is generally the most reliable.
264
265 The GMON, which is manufactured by Campbell Scientific (Canada) (CS7525;
266 http://www.campbellsci.ca/cs725), is composed of a tube 62 cm long, and 13 cm in
267 diameter, weighing 9 kg. The experimental set-up, which is illustrated in Fig. 1c, is based
268 on the initial, snow-free measurement of the number of counts for ^{40}K or ^{208}Tl per period
269 of time, which would be later decreased by the presence of the snowpack. Typically, 300

000 and 60 000 counts per 24 hours for ^{40}K and ^{208}Tl, respectively, are suggested as minimal values to provide accurate SWE measurements (CS725 Snow Water Equivalent Instruction Manual, 2017, Campbell Scientific [Canada] Corporation, Edmonton, AB; https://s.campbellsci.com/documents/ca/manuals/cs725_man.pdf). The observed rate of soil emission at each site allows the operator to define the minimum sampling time frequency. Seeding experiments conducted using potassium fertilizer show the potential for increasing potassium counts that are measured by the CS725 by up to 80% at sites where low counts are found (Wright et al., 2011). As is the case for ground-pointing CRNP, measuring the base-line signal of the radiation energy emanating from the ground prior to the first snowfall is a critical step in signal processing, given that it also depends upon soil moisture (SM) during the winter and spring periods. SM attenuates the natural dry-ground emission, resulting in an overestimate of SWE during signal processing when SM increases (Choquette et al., 2013) (see Sect. 4).

The CS725-Campbell GMON sensor has been the subject of a detailed performance analysis within the framework of the WMO Solid Precipitation Intercomparison Experiment (Smith et al., 2017). Moreover, since the device is sensitive to water contained in soils, it can be successfully used to estimate soil moisture during snow-free seasons. An operational GMON network, with a sampling frequency of 6 h, is actually deployed across the southern part of Québec and Labrador, northeastern Canada (45-55°N); it accounts for 116 stations that are operated by Hydro-Québec (87), Rio-Tinto's hydropower (Bauxite-aluminum smelters) (13), Ministère de l'Environnement et de la Lutte contre les changements climatiques of the Québec Government (10), Parks Canada (4), and the Government of Newfoundland and Labrador (2), and which are dedicated to water resource forecasting (Alexandre Vidal, Hydro-Québec, personal communication, November 2020). Also, these continuous measurements from the GMON Québec network are demonstrably very useful for validating the assimilation of microwave observations into a snow model (Larue et al., 2018). Recently, GMON had also demonstrated its robustness in a research project on seasonal snow monitoring from a station that was installed at 4962 m asl in the Nepalese Himalayas (Langtang Valley) to quantify the evolution of SWE (Kirkham et al., 2019).

2.3 FMCW radar (FMCW-Radar)

The principle of frequency-modulated continuous-wave (FMCW) radar has been well known since the 1970s (see the reviews by Peng and Li, 2019 and by Pomerleau et al., 2020) and has been popularized for snow studies since Koh et al. (1996), Marshall et al. (2005), and Marshall and Koh (2008), among others, were published. FMCW-Radar is an active system design for distance measurements. The radar emits a wave at variable frequencies that are centered on a reference frequency. When the radar receives a return from a target, the frequency difference between the emitted and reflected signals is measured (Fig. 1d). Since the frequency change rate is known, the time between the emission and the reception of the echo can be measured, from which the radar–target distance is calculated.

The principle of SWE retrieval is based on the time measurement of wave propagation in the snowpack that is proportional to the snow refractive index (square of permittivity), which changes the wave-speed propagation. As the refractive index of snow can be linked to its density (Tiuri et al., 1984; Matzler, 1996; Pomerleau et al., 2020), SWE can be retrieved knowing the snow depth. The experimental set-up is shown in Fig. 1d and illustrated in Fig. 2e.

Two main FMCW-radar specifications are required for SWE measurement: the radar central frequency and its bandwidth that is scanned. The central frequency specifies three parameters: a) the loss in signal strength of an electromagnetic wave that would result from a line-of-sight path through free space (the higher the frequency, the greater the loss); b) its penetration depth (the higher the frequency, the less penetration power it has); and c) its sensitivity to liquid water content in the snowpack. The bandwidth specifies the distance resolution and, thus, the precision: the wider the bandwidth, the lower the resolution. There is negligible frequency dependency of the snow refractive index (n'), which governs wave propagation in the snowpack. The refractive index (n') is linked to snow density (ρ) by a linear relationship: $n' = 8.6148 \cdot 10^{-04}\rho + 9.7949 \cdot 10^{-01}$ (Pomerleau et al., 2020).

For snow studies, several FMCW radars with different frequencies and resolutions are used, such as those common at the X-band (10 GHz), operating over 8–12 GHz (Ellerbruch and Boyne, 1980; Marshall and Koh, 2008). They provide a vertical resolution on the order of 3 cm. In contrast, L-Band FMCW radar (1.12–1.76 GHz) allows greater penetration but suffers from reduced vertical resolution (Yankielun et al., 2004). Multiband band FMCW radars have also been developed (Rodriguez-Morales et al., 2014), such as an L/C-band (2–8 GHz) that was used to successfully retrieve snow depth (Fujino et al., 1985), a C/Ku (8–18 GHz) large wideband FMCW radar that is capable of detecting crusts as thin as 0.2 mm within the snowpack (Marshall and Koh, 2005), or the improved (C-, X-, and Ka-band) radar (Koh et al., 1996). Operating frequencies of commercial, low-cost radar systems, such as those that are adopted for automotive radar systems (Schneider, 2005), are now available for K-band (24 GHz) and W-band (77 GHz) applications.

The availability of such new types of lightweight and very compact 24-GHz FMCW radar systems has motivated our research group to assess their ability to monitor the SWE continuously and autonomously (Fig. 2e) (Pomerleau et al., 2020). The FMCW-Radar that is used, which is centered on 24 GHz (K-band), is manufactured by IMST (IMST sentire™, IMST, Kamp-Lintfort, Germany; http://www.radar-sensor.com/); its housing module is very compact (114.0 mm × 87.0 mm × 42.5 mm) and weighs 280 g. This FMCW-Radar has a bandwidth of 2.5 GHz, scanning over 23–25.5 GHz, which provides a resolution of 6 cm in the air. These specifications appear to be a good compromise between penetration and resolution capabilities for SWE estimation, while keeping the sensor affordable, light and compact, with low power consumption. The radar penetration depth (δPr) of dry snow significantly decreases with density following a power law, which varies with temperature (see Fig. A2, Pomerleau et al., 2020). At T = 0 °C, δPr decreases from 6.78 to 4.81, 3.26

358 and 2.05 m for respective snow densities of 150, 200, 275 and 400 kg m^{-3} (Pomerleau et
359 al., 2020). Wet snow drastically reduces δPr, given that liquid water strongly absorbs the
360 radar signal, leading to high reflectivity at the air/wet snow interface and weak
361 transmissivity. For example, the two-way radar penetration depth decreases abruptly
362 from 2 m for dry snow at a density of 400 kg m^{-3} to 0.05 m for wet snow with 0.5% of
363 liquid water content (as a volume fraction). It should be noted that this strong sensitivity
364 to wet snow allows the radar to precisely detect the onset of snowpack surface melt, a
365 benefit that is discussed in Sect. 4.

366 One of the main interests of this approach is its potential capacity to estimate SWE from
367 a small remotely piloted aircraft (RPA). Over the Arctic, snow cover can generally be
368 characterized as a two-layer snowpack structure, which is composed of a dense wind-slab
369 overlaying a less-dense depth hoar layer (Rutter et al., 2019; Royer et al., 2021). Thus,
370 assumptions can be made regarding the mean refractive index of each of these layers,
371 thereby allowing SWE to be estimated (Kramer et al., 2021). Hu et al. (2019) also showed
372 the usefulness of imaging FMCW synthetic aperture radar onboard the RPA. Several
373 studies have also shown the potential of FMCW radar for different applications, such as
374 avalanche studies (Vriend et al., 2013; Okorn et al., 2014; Laliberté et al., 2021), snow
375 stratigraphy based on successive FMCW echo analyses (Marshall and Koh, 2005; Marshall
376 et al., 2007), snowpack tomography (Xu et al., 2018), and ice thickness monitoring
377 (Yankielun et al., 1993; Gunn et al., 2015). Pomerleau et al. (2020) obtained highly
378 accurate measurements of lake ice thickness using the 24 GHz FMCW radar, with a root-
379 mean-square difference (RMSD) of 2 cm accuracy up to ≈1 m ice thickness (derived from
380 35 manual in situ measurements).

381 2.4 GNSS receivers (GNSSr)
382 The principle of SWE retrieval based on Global Navigation Satellite System (GNSS)
383 receivers is to use the signals that are emitted at 1.575 and 1.609 GHz. by the GNSS
384 satellite constellations. SWE can be related to the carrier phase change that is induced by
385 the delay caused by the snowpack at ground level. With two static receivers (standard
386 GNSS antennas), i.e., one placed under the snow and the other above the snow, carrier
387 phase measurements of both receivers can be compared and SWE derived using the
388 onboard measurement hardware (Fig. 1e) (Henkel et al., 2018). Comparing GNSS signal
389 attenuation measurements at the two antennas (below and above the snowpack) also
390 permits the retrieval of Liquid Water Content (LWC) of the wet snow (Koch et al., 2019).
391 Snow depth retrieval has been operational for longer, based on interferometric
392 reflectometry of GNSS signals (see Larson et al. 2009; Larson, 2016). Steiner et al. (2019)
393 used a slightly simplified retrieval algorithm based on the path delay estimates of the GPS
394 signals while propagating through the snow cover due to both refraction at the air-snow
395 interface and decrease in wave velocity in the medium.
396
397 This relatively recent and novel approach has been validated (Henkel et al., 2018; Steiner
398 et al., 2018; Koch et al., 2019; and Appel et al., 2019). A system has now been
399 commercialized by VISTA Remote Sensing in Geosciences GmbH, Munich, Germany

(SnowSense©, https://www.vista-geo.de/en/snowsense/). The experimental set-up is described in Fig. 1e, based on a low cost and lightweight system. In this study, we used the SnowSense system for monitoring SWE and LWC throughout a winter, together with other sensors (see Results Sect. 3). We also developed our own system, shown in Fig. 2d.

Another promising way to monitor SWE, which is based on the same principle of GNSS, is the use of powerful satellite transmissions as illumination sources for bistatic radar. This so-called "Signals-of-opportunity (SoOp)" approach covers a wide range of frequencies, such as emissions from United States Navy Ultra High Frequency (UHF) Follow-On (UFO) communication satellites in P-Band frequencies (between 240-270 MHz). From two P-band antennas (one direct and one reflected), Shah et al. (2017) demonstrated the feasibility of retrieving SWE using the phase change in reflected waveforms, which is linearly related to the change in SWE. These methods were not included in this review since they are still in the development stage and not sufficiently mature to be operational.

3. Results

Continuous and simultaneous recordings of different instruments on different sites were analyzed to evaluate their behavior in terms of their temporal evolution. Manual measurements were used to compare the data between them. First (Sect. 3.1 and 3.2), two experiments we conducted were compared: GMON and CRNP (Sect. 3.2.1); and GMON, Radar and GNSSr (Sect.3.2.2). A comprehensive literature review and evaluations of similar sensors are then presented in Sect. 3.3. This later section also includes uncertainty estimates of our experiments and from this review, which are synthesized in Table 2.

3.1 Experimental sites and methods
We compared four instruments at two snow research stations that were located in Québec (Canada). The first was the SIRENE site (Site Interdisciplinaire de Recherche en ENvironnement Extérieur), which is situated on the main campus of the Université de Sherbrooke in a temperate forest environment (45.37°N, -71.92°W, 250 m asl) (Fig. 2d). The second site is the NEIGE-Forêt Montmorency (NEIGE-FM) research station. The instruments were located in an open area (Fig. 2e) of the Montmorency experimental forest (47.32° N; -71.15° W, 640 m asl) of Université Laval (Quebec City), which is in the boreal forest. The NEIGE-FM snow research station is part of the World Meteorological Organization (WMO) Global Cryosphere Watch (GCW) Surface Network CryoNet (http://globalcryospherewatch.org/cryonet/sitepage.php?surveyid=191).

Two methods were used to obtain in situ manual SWE measurements in the vicinity of the four SWE-systems: the snowpit (SP) approach; and snow-tube core samplers (see Kinar and Pomeroy, 2015; López-Moreno et al., 2020). The SP-based SWE values (in mm w.e. = kg m^{-2}) were derived from vertical continuous density profiles, which were determined by weighing snow samples at a vertical resolution of 5 cm (height of the density cutter). Assuming an accuracy of density cutter measurements of about 9%

444   (Proksch et al., 2016), the mean relative SWE accuracy from snowpit can be estimated to
445   be of 6–12%. SWE estimates were also obtained by weighing the extracted core sample
446   of known diameter (Ø) and snow depth using a coring tube. In this study, the core
447   sampling was performed using three different snow tube models, which were averaged:
448   "Carpenter" (Federal standard sampler, 3.7 cm Ø tube), the Hydro-Quebec snow tube
449   (12.07 cm Ø), and an in-house Université Laval snow tube (15.24 cm Ø). The uncertainties
450   of tube core sampling that we carried out on snowpack up to 600 mm SWE with large
451   tubes is on the order of 6%, but can be higher, up to 12%. Such uncertainty is difficult to
452   define, as discussed in Sect. 3.3 and in the Appendix. Furthermore, as manual
453   measurements cannot be taken at the same location throughout a given winter period,
454   this could generate uncertainty when compared to a fixed instrument, due to small-scale
455   spatial variability of SWE and surface roughness (López-Moreno et al., 2020).
456
457   The snowpack properties were derived from GMON and CRNP systems throughout the
458   entire winter season of 2008-2009 (Fig. 3) and from GMON, FMCW-Radar and GNSSr
459   systems in 2017-2018 (Fig. 4). The CRNP probe that was used was the same as the French
460   EDF probe that was placed on the ground (Paquet et al., 2008) and installed at about 5 m
461   distance from the GMON footprint. The GMON was installed on a 2 m mast above the
462   surface, located in a slight depression in comparison with the terrain where the CRNP was
463   buried. The CRNP counts were accumulated over 1 hour and normalized against an
464   identical probe that was installed nearby, just above the snow surface. The GMON counts
465   were accumulated over 6 hours, and only ^{40}K counts were considered (TI counts were
466   similar, but not shown). The GMON sensor was adjusted to take into account the soil
467   moisture prior to snowfall accumulation, but not afterwards.
468
469   In addition to SWE measurements, continuous automatic snow depth measurements
470   were performed using an ultrasonic ranging sensor (Campbell Scientific, SR50AT-L), and
471   manually with a graduated probe around the sampling sites. LWC measurements were
472   derived from GNSSr (Fig. 4). Air temperature (T) at 2 m height and total daily precipitation
473   (tipping bucket rain gauge) were recorded at the SIRENE site; a threshold of T = 0 °C was
474   used to separate solid and liquid phases.
475   In this section, we present comparisons between these sensors with manual snowpit
476   validation data that were measured as close as possible to the automatic instruments.
477   The uncertainty of measurements, including other measurements that we carried out
478   (not shown), is reported in Table 2.
479
480   3.2 Validation of measurements
481   3.2.1 Comparison of GMON- and CRNP-derived SWE seasonal evolution
482   Figure 3 shows the SWE evolution of a shallow snowpack (maximum snow depth of 56
483   cm) at the SIRENE site that was derived from daily mean values of the GMON and CRNP
484   data throughout the winter season of 2008-2009.
485
486   Results show that GMON and CRNP evolve similarly over the winter, with GMON SWE
487   being slightly higher after the first winter month (SWE > 50 mm). This difference occurred

after a pronounced melting spell (29-30 December 2008) and is explained by the water that has accumulated on the ground under the GMON and not on the CRNP, due to the local terrain configuration. The moisture beneath the GMON formed a significant ice layer that lasted all winter. As this ice layer was not present in snowpits (the amount of water in an ice crust being otherwise difficult to measure), this could possibly explain differences between GMON and manual measurements. Precipitation data (snowfall and rain) show how GMON and CRNP evolve with each event (Fig. 3). But for studying short meteorological events, the measurement period linked to a given instrument should be short enough to be able to account for rapid changes in SWE. This can be seen in Fig. 3 showing higher variability in SWE derived from CRNP based on counts accumulated over 1 hour than those derived from GMON based on counts accumulated over 6 hours. Moreover, small snowfalls on top of a thick (denser or wet) snowpack were not always detected. Further studies are needed to address challenges related to sub-daily reliability of these instruments.

For that given winter, rain-on-snow events were frequent, leading to moisture accumulation on the ground. Note also that at the end of the winter, there was ice that had not yet melted and water accumulation under the GMON, resulting in a significant GMON overestimation in terms of SWE but not in terms of total water (snow + ice). There was no more snow on the ground after 20 March 2009. The accuracy measurements are discussed in Sect. 4.2.
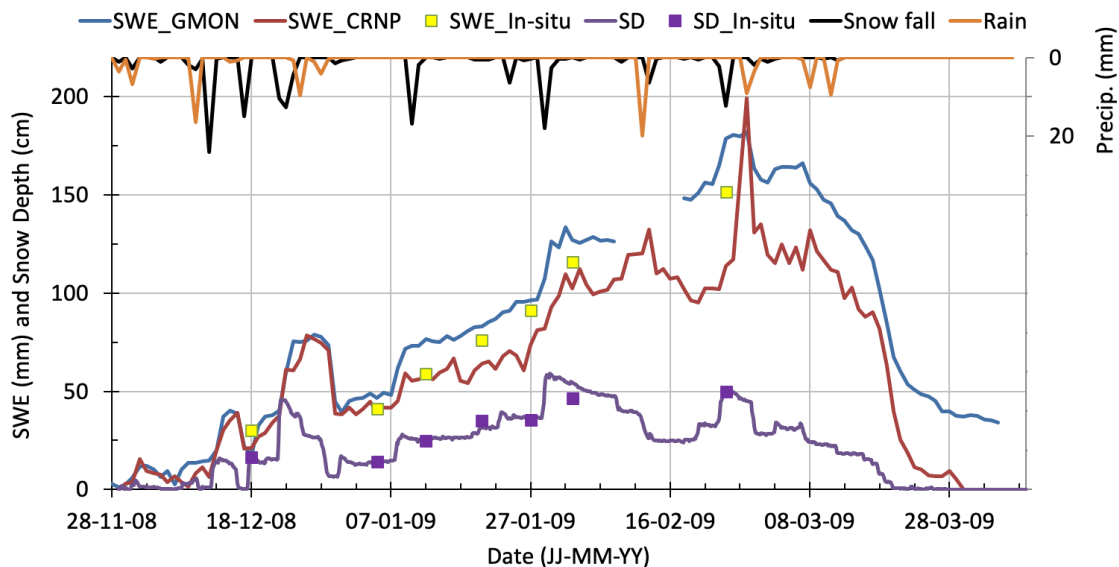

Figure 3. GMON- and CRNP-derived Water equivalent of snow cover (SWE, mm w.e.), snow depth (SD, cm), and recorded daily solid and liquid precipitation (Precip., mm, right hand scale), in comparison to validation data (in situ) at the SIRENE site for the winter season of 2008-2009. Continuous SD measurements (purple line) are from SR-50 and SD_in situ measurements (purple square) are from snowpits. Open yellow squares correspond to manual in situ SWE measurements.

518 3.2.2 Comparison of GMON-, Radar- and GNSSr-derived SWE seasonal evolution
519 Figure 4 shows the SWE evolution that was measured by the three instruments: GMON
520 (^{40}K counts only), FMCW-Radar and GNSSr, which had been placed in close proximity to
521 one another at the NEIGE-FM research station for the winter season of 2017-2018. A
522 maximum snow depth of 120 cm was measured during the season, corresponding to a
523 SWE maximum of 500 mm w.e. at the end of April.
524
525 The three instruments were compared to manual in situ measurements that had been
526 derived from SP (red squares) and core (red triangles) approaches in Fig. 4. We
527 distinguished the two methods (SP and snow core) because they exhibit significant
528 differences, with a RMSD of 33 mm (12%). These discrepancies are the result of two
529 problems: 1) SWE spatial variability, mainly due to snow depth variability (López-Moreno
530 et al., 2020); and 2) the method that was used, since the design of snow tubes and cutters
531 has some influence on sampling errors and bias (Goodison et al., 1987; see Appendix).
532 Therefore, uncertainty analyses (Sect. 3.3) were performed considering manual SP as the
533 reference because the SP approach was used for both experiments.
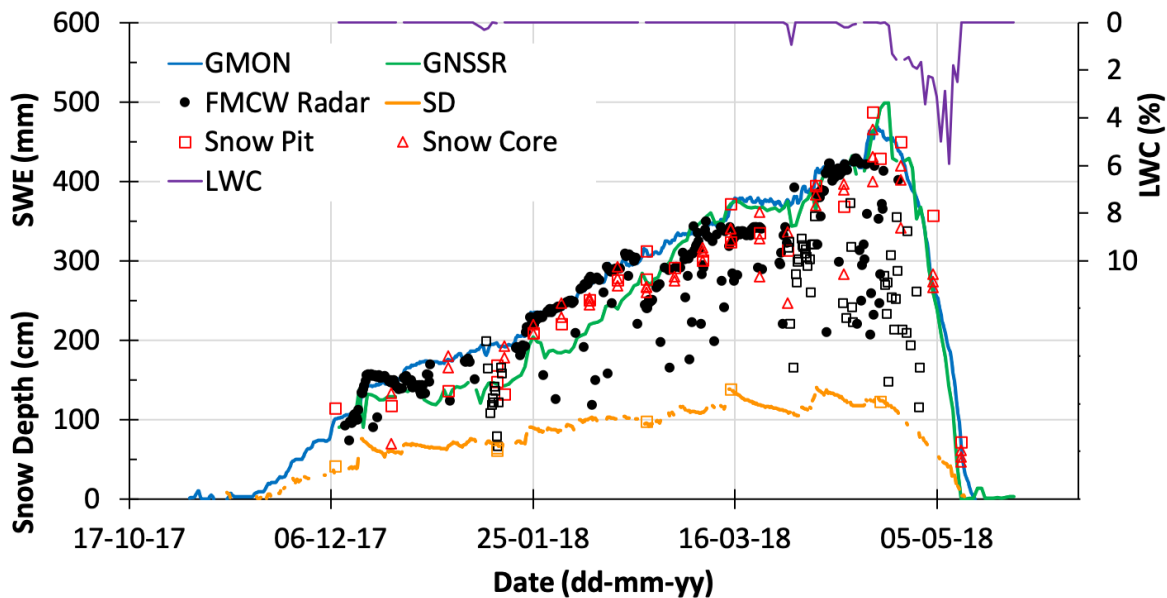534
535

536
537 Figure 4. GMON- (blue line), FMCW Radar- (black closed circles) and GNSSr-derived (green
538 line) Water equivalent of snow cover (SWE, mm w.e.), snow depth (orange line for
539 SR50AT-L data and orange open squares for in situ data) (SD, cm) and GNSSr-derived
540 Liquid Water Content (LWC, % volumetric, purple line, right scale), in comparison to in
541 situ snowpit (open red square) and snow core (open red triangle) SWE measurements at
542 the NEIGE-FM site for the winter season of 2017-2018. For FMCW-Radar data (in black),
543 plain circles are for dry snow, while open squares correspond to wet snow.
544
545 The continuous simultaneous recordings from the different instruments permit temporal
546 evolution analysis (Fig. 4). During the accumulation period, GMON shows relatively

15

547 smooth and consistent evolution in SWE leading to a maximum of 465 mm on 19 April
548 2018, while the FMCW-Radar time series is more erratic and requires filtering to remove
549 low SWE outliers. These points are mainly due to incorrect detection of the peak of the
550 radar echo on the ground (snow-ground interface), sometimes with low amplitude, and
551 which can be filtered with improved data quality processing of raw recording (Pomerleau
552 et al., 2020). In particular, all data that were acquired under wet snow conditions (open
553 black squares, Fig. 4), which correspond to melting periods with measured air
554 temperature above 0° C, are obviously underestimated as expected, because of radar
555 wave absorption by liquid water in the snowpack. Compared to the GMON, the GNSSr
556 signal increases with values that are lower than the GMON until mid-March at which point
557 it continues to evolve with similar values, as the GMON SWEmax of 499 mm w.e. was
558 reached on 23 April 2018. The behavior of the three instruments, showing different
559 patterns of snow evolution, always remains close to in situ observations (RMSE compared
560 to the snowpit for GMON and GNSSr are respectively 34 mm and 32 mm; Table 2). It
561 should be noted that in Fig. 4, there is a small difference (+4 days) between the
562 disappearance of snow cover that was recorded with GNSSr (11 May 2018) compared to
563 GMON (14 May 2018). The GNSSr sensor is not sensitive to soil moisture, while GMON is,
564 despite the instruments being located on a well-drained sandy site (NEIGE-FM site). In the
565 case shown here, the end of snowmelt is well captured by both instruments. The accuracy
566 between instruments is analyzed in Sect. 3.4, including a second winter season of
567 continuous measurements at the NEIGE-FM site (2016-2017, Pomerleau et al., 2020).
568
569 GNSSr also measures the Liquid Water Content (LWC) of snow (purple line in Fig. 4). The
570 non-zero LWC values correspond well to positive air temperatures that were recorded at
571 this site, and also to the drop in FM-Radar measurements (open black squares).
572
573 3.3 Analysis of measurement uncertainty
574 It is challenging to compare the accuracy of several instruments, given that there is no
575 absolute reference for estimating SWE (see Kinar and Pomeroy, 2015). In situ manual
576 measurements are themselves subject to error, with varying precision depending upon
577 the method that is being used. Errors are incurred that depend upon the types of density
578 cutter, tube diameter, sampling quality that is operator dependent, and ice lenses in the
579 snowpack, among other sources. This is a long-debated topic, with no actual established
580 international standard protocol (Work et al., 1965; Goodison et al., 1981, 1987; Kinar and
581 Pomeroy, 2015, López-Moreno et al., 2020). Commonly, the relative uncertainty for SWE
582 measurement using snow core varies from 6% for shallow snowpack (0-300 mm w.e.), to
583 8% (300 – 1000 mm w.e.) for medium snowpack to 10-12 % for deeper snowpack (> 1000
584 mm w.e.) (see discussion in Appendix). Moreover, because manual measurements cannot
585 be taken at the same location during a given winter period, uncertainty can be introduced
586 by well-known local spatial variability of snow depth that can occur at fine scales around
587 the sensors. Such variability depends upon several factors, such as the region and the
588 environment (Arctic area, aspect and slope in mountainous areas, for example), the
589 micro-topography and roughness, the vegetation, and snow redistribution by the wind
590 (Clark et al., 2011; Bormann et al., 2013; Rutter et al., 2014; Meloche et al., 2021; Royer

591 et al., 2021). Furthermore, temporal variability of snow depth and SWE during the winter
592 requires regular validation measurements throughout the season.
593 The sensor uncertainties were evaluated from results of our experiments (Sect. 3.2) and
594 from published studies at other experimental comparison sites (this section). These other
595 sites are: the Weissfluhjoch high-alpine site near Davos, Switzerland (46.83° N, 9.81° E, 2
596 536 m asl); Sodankylä, Finland (67.37° N, 26.63° E, 185 m asl); Caribou Creek, SK, Canada
597 (53.95° N, -104.65°W, 519 m asl); and Fortress Mountain ski area, Kananaskis Country,
598 Canadian Rocky Mountains, AB (50.82° N, -115.20° W, 2 330 m asl). We also conducted a
599 series of manual FMCW-radar measurements (e.g., instrument operated by hand, rather
600 than automatically) over dry snowpack and compared them with in situ SWE
601 measurements over a wide range of conditions (snow depth and density) in boreal forest
602 (47° N, 18 points), subarctic taiga (54–56° N, 32 points) and Arctic tundra (69° N, 28 points)
603 environments along a northeastern Canadian transect (Pomerleau et al., 2020).
604 Note that we only consider here the differences between instruments in the field and do
605 not address accuracies that were derived from instrument calibration by the
606 manufacturer.
607
608 Table 2 summarizes the uncertainties of each instrument and protocol (five cases: CRNP
609 in and above ground, GMON, FMCW-Radar and GNSSr) in relation to in situ manual
610 measurements (snowpit method), as well as against snow pillow and snow scale data that
611 were considered as reference measurements by the authors of the publications
612 consulted. The results from the COSMOS-UK network (Wallbank et al., 2021) were not
613 included in the overall uncertainty analysis, because, in this study, depth-based SWE
614 estimate of fresh snow was used to assess the uncertainty of CRNP (R^2 of 0.53, in the
615 range of 0-40 mm w.e.). Moreover, soil moisture is usually high and variable in UK, which
616 acts to increase uncertainties in the SWE estimate (Wallbank et al., 2021).
617 Even if the mechanical method is well known and has been proven over many years, the
618 snow pillow can sometimes generate large errors when bridging processes occur that are
619 linked to freeze–thaw cycles leading to disconnection of the weighing mechanism of the
620 overlying snowpack and the surrounding snowpack (Kinar and Pomeroy, 2015). However,
621 to compare measurements at a daily scale, they are worth looking at. In Table 2, the
622 uncertainty that relates to the characterization of measurement dispersion compared
623 to a reference was defined, when known. We used the root-mean-square difference
624 (RMSD) between an instrument and a given reference, and by a linear regression over the
625 whole range of measured SWE data that was defined by the coefficient of determination
626 (R^2), the slope and the intercept. The number of points is also given.
627
628 Table 2 here
629
630 Uncertainty analysis does not allow us to determine the "best" instrument, due to the
631 diversity of experimental conditions, including the range of SWE, the number of
632 experimental sites and point measurements, and the analyses that are performed over
633 one or several seasons. It appears that all five methods show a RMSD in the range of 14
634 to 48 mm (mean 33 ± 11 mm) against in situ snowpit manual measurements (Table 2).

635   This represents a relative value of around 12% on average, depending on the instruments.
636   The mean coefficient of determination for the linear regression is also substantially high
637   (mean R^2 = 0.92 ± 0.07). Calculated average slope is 0.976 ± 0.13, meaning that in general,
638   the instruments slightly underestimate SWE for higher SWE values compared to in situ
639   measurements, even if this is not always the case (Table 2). RMSD increases slightly when
640   the analysis was performed over a deep snowpack (0–1000 mm w.e.) and decreases when
641   compared to another continuous instrument instead of manual data (instrument vs
642   GMON and instrument vs snow pillow, average RMSD = 23 ± 10 mm, Table 2).

643

644   For the GNSSr instrument that allows the operator to differentiate dry from wet snow,
645   Koch et al. (2020) have shown that SWE RMSD is about 2.4-fold higher for wet snow than
646   for dry snow. They did not provide information on LWC uncertainty. In late winter 2021,
647   for very wet melting snow, we did a validation measurement using the WISe A2 Photonic
648   probe (snow liquid-water content sensor that is based on snow microwave permittivity
649   measurements; https://a2photonicsensors.com/wise/). The GNSSr LWC was of 0.44 % (in
650   volume) (the retrieved GNSSr SWE was 149 mm w.e) and the LWC from the in situ probe
651   was of 0.47 % for the upper half of the snowpack. The snowpack SWE that was measured
652   manually was 133 mm. The lower half of the snowpack was saturated with water. The
653   uncertainty in wet SWE retrieval could result from approximations in the retrieval
654   algorithm that is used. For example, the wet snow refractive index varies linearly with
655   LWC, with a slope significantly dependent of the snow density (see the appendix of
656   Pomerleau et al., 2020). This aspect could probably be addressed further by improved
657   inversion.

658

659   The uncertainty comparison in Table 2 must be weighted according to the analysis
660   conditions. The accuracy estimates can actually depend upon the number of points being
661   used and their distribution over time. High inter-annual variability of the snowpack state
662   (see Bormann et al., 2013; Lejeune et al., 2019) ideally would necessitate several years of
663   measurements over the winter. The uncertainties of each GMON and CRNP instrument
664   were derived from huge data sets that were based on operational networks from the
665   GMON Hydro-Quebec network in Canada and the Alps' EDF network for the CRNP,
666   respectively, with a very large number of samples taken over several years of experiments
667   and from multiple sites. The accuracy of the GMON that is given by the manufacturer is ±
668   15 mm for SWE < 300 mm and ± 15% for SWE of 300-600 mm, which is probably rather
669   conservative. When SWE reference data and site adjustment process are well done, the
670   GMON is able to report SWE with an <u>uncertainty</u> as low as 5% (Wright, 2011; Choquette
671   et al., 2013; Wright et al., 2013). The accuracy of the SnowFox sensor (CRNP) that has
672   been provided by the manufacturer (5-10%) must be confirmed. The GNSSr approach has
673   recently been the subject of two different comparative analyses showing very promising
674   results (Henkel et al., 2018; Koch et al., 2019), which were confirmed by our own results.
675   Over a full season, we obtained an excellent relationship between GNSSr and in situ
676   manual measurements (relative RSMD = 11%, Table 2) and compared with GMON (RMSD
677   = 34 mm, 12%, SWE_{GNSSr} = 1.126 SWE_{GMON} - 59.3, R^2 = 0.97, 153 days).

678

4. Strengths and Weaknesses of Instruments

In this section, we review the advantages and drawbacks of each of the instruments that are presented, summarized in Table 3. This analysis is based on our experience on instruments and their performances, and a literature review on experimental results of measurements that were carried out with the same approaches. We only consider these field sensors for SWE measurements in terms of their continuous and autonomous capacities, from the perspective of an operational networking context, including criteria regarding low maintenance and relatively easy installation without requiring heavy infrastructure. The four instruments that we analyzed are: CRNP with two experimental setups, i.e., instrument in the ground and above the snow; GMON; 24-GHz FMCW-Radar; and GNSSr (see Table 1 for acronyms and Fig. 1 for the experimental setup). They are all capable of working on batteries and solar panels, by adjusting, if necessary in certain cases, the measurement protocol, i.e. by reducing the frequency of acquisition and on-board data processing. Ten criteria were considered (Table 3): - the SWEmax capability; - other measured parameters; - whether ancillary data were required for SWE retrieval; - the temporal sampling rate, i.e., whether they were capable of quasi-continuous SWE measurement capability, although the notion of continuous SWE measurements is relative to the application; - the footprint of the sensor, i.e. taken here in the sense of the area from which emanates the measured radiation having interacted with the snow; - the power consumption; - the main strength of the approach; - their critical drawbacks; - the price of the instrument itself, knowing that the cost of the system may vary in case additional instruments are required for the SWE measurements. Also, the cost that is associated with on-site maintenance during winter should be considered here, but in our case, the 4 instruments are considered on the same basis, i.e., autonomous, with no need for intervention; - and the possibility of other applications.

The cost criterion is a very relative argument, which can influence the choice of decision-makers or researchers, depending upon the intended application (e.g., large network, in remote areas, among others) and also on the purchasers.

Table 3 here

To complement the main criteria that are presented in Table 3, we include the following additional considerations, which are reported in the literature, by order of presentation rather than order of merit.

The CRNP approach is based on neutron component that has absorption mean free path about an order of magnitude larger than that for gamma radiation. This makes it the most efficient system for very deep snowpack analysis (Paquet et al. 2008). Measurements of snowpack of up to 2000 mm SWE were performed using the SnowFox sensor at the UC Berkeley Central Sierra Snow Lab in Soda Springs, CA (2120 m asl;).

722   Regarding CRNP above the snow, Schattan et al. (2017) estimated the theoretical winter
723   footprint over snow, which they defined as the distance from where neutrons originate.
724   They found that 86%, 63% and 50% of neutrons originate within respective distances of
725   273, 102, and 49 m. In practice, the authors found that the average footprint during the
726   season, based on measurements over almost three snow seasons, was estimated to be
727   around 230 m, possibly more.
728
729   Moreover, CRNP is inherently weakly sensitive to interference from vegetation compared
730   to systems that are based on EM low frequencies (GMON, FMCW-Radar and GNSSr). This
731   is in part because the attenuation coefficient for fast neutrons ($\sim$0.01 m^{-2} kg in water,
732   Murray and Holbert, 2020) is an order of magnitude smaller than the analogous
733   attenuation coefficient in vegetation for GNSS microwaves (1.5 GHz) (e.g., Wigneron et
734   al., 2017). Also, vegetation can itself be a significant source of electromagnetic emissions
735   (Larson et al., 2014; Wigneron et al., 2017). The CRNP is affected by all sources of
736   hydrogen within its measurement footprint. As Biomass increases the hydrogen
737   concentration in the CRNP's footprint, it is possible to monitor changes in biomass (Vather
738   et al., 2020).
739
740   The instruments pointing toward the soil, CRNP and GMON above the surface, are
741   sensitive to soil moisture. This can be a relatively large source of error with these
742   measurement principles, given that these sensors are interpreting near-surface soil liquid
743   content as SWE. This is especially the case during spring freshets and mid-season thaw
744   cycles (see Fig. 3 and Smith et al., 2017). Heavy rainfall on snow also leads to erroneous
745   SWE estimates due to the occurrence of water ponding beneath the snow (Fig. 3).
746   Installation on well-drained soils can mitigate these effects, as shown in Fig. 4. By
747   assuming that soil moisture levels remain stable throughout winter, which can be the case
748   when soil remains frozen (see Gray et al., 1985, 2011), this soil moisture-induced bias can
749   be adjusted prior to the first snowfall or one must apply a correction based on soil
750   moisture conditions that are otherwise known. Based upon 10+ years of experience with
751   a large GMON network that is deployed in Québec, Canada, over northern organic boreal
752   soil, it has been shown that in most cases, SM does not vary substantially during the
753   winter season (Choquette et al., 2013; Ducharme et al., 2015). To consider SM as
754   constant, mathematical equations that are used in calculating SWE can be simplified. If
755   the goal is to measure the total water that is available for hydrological purpose, this
756   aspect can become an advantage.
757
758   Counter-based sensors such as CRNP and GMON need to accumulate enough counts for
759   reliable SWE estimates. Thus, it may be necessary to accumulate the counts over an
760   adjusted period of time (several hours, depending on the case), so that the measurement
761   is not strictly continuous. This can prevent accurate detection of short events, sudden
762   heavy snowfalls, for example.
763
764   For the GMON, depending on the type of soil at the measurement site, gamma ray
765   emissions may not be sufficient and could require a longer integration period, as is the

766   case for sites with thick organic soil layers. It is possible to enrich gamma emissions by
767   using bags or pipes of potassium-rich fertilizer, thereby maintaining a shorter integration
768   time. Wright et al. (2011) achieved success with this approach, which yielded significantly
769   higher count strengths. Such a protocol is illustrated in Fig. 2g (data not yet processed).
770   Over glaciers, GMON requires such an enriched gamma emission setup. The size of the
771   area that is effectively monitored by the GMON ("footprint") extends to 10 m from the
772   detector when there is no snow or water on the ground (Ducharme et al., 2015). The size
773   of the sensed area exponentially decreases with increasing SWE and is estimated to be
774   of the order of 5 m radius (50 − 100 m^2) for 150-300 mm w.e. (Martin et al., 2008;
775   Ducharme et al., 2015). This relatively large foot print is an advantage of this sensor.

777   With FMCW-Radar technique, as previously stated, penetration depth strongly depends
778   on the measurement frequency. Generally, high frequency instruments result in higher
779   resolution measurements, but these are also affected by greater signal attenuation, i.e.,
780   by a reduced depth of penetration. A disadvantage of this approach is that it requires the
781   measurement of snow height as close as possible to the radar sensor. Also, the algorithm
782   for thresholding the radar echo peaks must be developed as well as the calculation of the
783   SWE (see Pomerleau et al., 2020).

785   GNSS electromagnetic waves can be attenuated under the forest canopy, as the forest
786   transmittivity at 1.5 GHz is not negligible (Wigneron et al., 2017). Yet, because we
787   normalized the signal beneath the snow against the one acquired above the snowpack,
788   when both antennas were placed under the canopy, this effect should not alter retrieval.
789   GNSSr is not well suited to very steep mountainous terrain (e.g., deep-valley bottoms),
790   given that a rather wide sky-view factor is needed by the instrument, and that this view
791   can be limited in such environments, depending on slope and location (Koch et al., 2019,
792   Steiner et al., 2018).

794   The main conclusions that emerge from Table 3 and the aforementioned remarks are the
795   following, recalling that each approach has its own advantages and limitations (by order
796   of presentation rather than by order of merit):
797   •   The CRNP approach is based on measurements of natural cosmic ray fluxes, which are
798   variable in time, unfortunately requires complementary atmospheric measurements
799   (temperature, pressure and atmospheric humidity) at each site for correcting the
800   signal and must be normalized against a nearby reference site (available worldwide).
801   <u>CRNP on </u>the ground: This is the most efficient system for very deep snowpack (> 2000
802   mm w.e., perhaps up to 7000 mm w.e.), as is the case in mountain environments or
803   northerly areas that are witness to winter lake-effect snowfall. The most
804   advantageous aspect of the CRNP is its ability to measure SWE through complex snow
805   layers from shallow to deep snow conditions. This is a robust and mature approach,
806   as demonstrated by the French EDF experience (Gottardi et al., 2013; Lejeune et al.,
807   2019); however, the EDF's sensor is based on a system that is not exploited
808   commercially. The alternative sensors are the CRNP-based sensor that is
809   manufactured by Hydroinnova (SnowFox or CRS-1000/B, Hydroinnova, Albuquerque,

NM) (https://hydroinnova.com) and the CRD manufactured by Alpine Hydromet (www.alpinehydromet.com) and marketed by Geonor Inc. These sensors are relatively new and still need to demonstrate their robustness. The cost of Hydroinnova system is about 11 000 US$ for sensor only. As previously mentioned, ancillary sensors (atmospheric humidity and barometric pressure sensors) must be added, and the actual price could be up to 17 000 US$ for full setup. The cost of the Geonor Inc. system is 15 000 US$.

- CRNP above the snow: The most interesting system for measuring SWE over a large footprint, but it is limited to shallow snowpacks. It is the only approach that can provide an integrated spatial measurement. This approach also needs appropriate adjustment for each site in terms of soil moisture corrections, which can be difficult over a large area.

- GMON: This is one of the most mature instruments for snowpacks that are not too deep (600 mm w.e. according to manufacturer specifications, but up to 800 mm w.e based on our experience), with a medium footprint (10 m). Yet, it needs systematic site adjustment for soil moisture-induced error, which can increase the bias of measurements, particularly at the end of the winter when the soil becomes potentially saturated during snowmelt. It is the most expensive of the four instruments (around 16 600 US$, 20 000 $CAD). This system has proved its robustness and accuracy within the operational Hydro-Quebec Canadian network over a wide variety of environments for almost 10 years (Choquette et al., 2013).

- FMCW-Radar: This approach requires the measurement of the snow depth to be able to retrieve SWE. Its weak point is its limitation in measuring the SWE of wet snow. Yet, the instrument is very useful for dry snowpack characterization, in terms of stratigraphy or for avalanche studies, and also for detection of snowmelt events. Moreover, it is not expensive (1 000 US$, 800 €). As it is very light weight and compact, one of its strengths is its potential capability to retrieve SWE from remotely piloted aircraft above arctic snowpacks.

- GNSSr: The potential of the GNSSr approach, which is a light and compact system, is strong, given its capability of measuring SWE and LWC with high accuracy, and to derive snow depth. For SWE retrieval, its performance remains very good (relative RSMSD of ~10% in the range of 0-1000 mm) and has the capacity to measure deep snowpack (up to 1 500 mm w.e.). SWE accuracy for wet snow has yet to be improved, as it depends upon the GNSS signal processing. Its cost is 8 550 US$ (7 000 Euros). The station includes the software/license and processing is performed onboard of the station. The Station comes with 1 year of Iridium communication for retrieved product SWE/LWC (via VISTA). VISTA supports customer to find operational way to retrieve data in operational use for future. The license alone for processing the raw data can also be directly purchased at ANavS (https://anavs.com/) for 2 370 US$ (2 000 €).

5. Conclusions

In this paper, we evaluated four types of non-invasive sensors that have all reached a certain level of maturity enabling deployments of autonomous networks for monitoring Water equivalent of snow cover (SWE). These include the Cosmic Ray Neutron probe (CRNP), the Gamma Ray Monitoring (GMON) sensor, the frequency-modulated continuous-wave radar at 24 GHz (FMCW-Radar), and the Global Navigation Satellite System receiver (GNSSr) (see Table 1). This new generation of light and practical systems that are based on radiation-wave measurement is now commercially available. The GMON is already operationally used in Québec, Canada, for hydrological purposes (Hydro-Québec, Rio-Tinto, and governments).

The analysis of their performances that are summarized in Tables 2 (uncertainties of measurement) and 3 (pros and cons) show that each approach has its strengths and weaknesses. The synthesis of their advantages/disadvantages shows that the overall uncertainties remain in the range of manual measurements, i.e., 9 to 15%. CRNP that is placed in the ground beneath the snow is the only system capable of measuring very deep snowpacks, while the GNSSr sensor is limited to SWE up to ~1500 mm w.e., and the two others up to ~800 mm w.e.. Both CRNP and GMON approaches need systematic site adjustments for soil moisture characterization. In addition to SWE, an advantage of the sensor to be considered is its ability to measure other parameters, such as snowpack stratigraphy for the FMCW-Radar, and the liquid water content for the GNSSr. The GNSSr approach, which has relatively low cost and is light and very compact, appears to have a great potential in remote and difficult to access areas.

The requirement of automatic instrumentation networks for SWE measurements to improve seasonal snowpack monitoring is important for several applications, where spatially distributed SWE instruments are needed such as in remote and mountainous areas, for operational water resource and flood management over snow-driven watersheds. Networks of continuous SWE measurements are also required for calibrating satellite-derived SWE information, or for winter transportation safety. This review of continuous-monitoring SWE sensors is intended to help researchers and decision makers choose the one system that is best suited to their needs.

895 Charles Fierz, SLF, Davos; Yves Choquette, formerly of IREQ-Hydro-Québec; Florian Appel,
896 VISTA; and Reinhard Kulke, IMST.
897
898

906

907 **Conflicts of interest:**
908 The authors declare absolutely no conflicts of interest or business relationships with any
909 of the manufacturers that are mentioned in this article. The mention of commercial
910 companies or products does not constitute a commercial endorsement of any instrument
911 or manufacturer by the authors.
912
913

Table 2 Uncertainty analysis for the 4 systems that were considered. The Range measurement indicates the highest SWE (mm) value on which the analysis was performed. RMSD: Root Mean Square Difference. R² is the determination coefficient of the linear regression analysis. Pts: number of in situ manual samples. "-" means no information available.

Sensor	Reference data	SWEmax (mm w.e.)	Uncertainty RMSD (mm w.e.) (relative RMSD in %), R² (slope, intercept mm w.e.)	References, sites, number of points
CRNP in the ground	Manual snowpit	200	14 mm, R² = 0.96 (0.78, 8.5 mm)	This study (Fig. 3), 7 pts
	GMON	200	28 mm, R² = 0.89 (0.79, -3.9 mm)	This study (Fig. 3), 2008-2009 season
	Manual snowpit	1700	–, R² = 0.98 (0.99, 2.8 mm)	Gottardi et al. (2013) EDF system, Alps and Pyrénées 320 year.sites, 1037 pts.
	Snow core	2500	– (2% ± 13%), R² = 0.943 (–,–)	Gugerli et al. (2019), Glacier de la Plaine Morte, Switzerland, 9 pts (2 winters)
	–	–	5 – 10%	Hydroinnova snowFox[1]
CRNP above snow	–	–	5 – 10%	Hydroinnova CRS-1000/B [2]
GMON	Manual snowpit	500	34 mm (12%), R² = 0.93 (0.997, 17.1 mm)	This study (Fig. 3 and 4) and Pomerleau et al. (2020), SIRENE et NEIGE-FM, 64 pts
	Snow core	200	40 mm, R² = 0.92 (1.16, 16.8 mm)	Smith et al., 2017, Sodankylä, Finland, 30 pts
	Snow core	125	23 mm, R² = 0.90 (0.904, 27.5 mm)	Smith et al., 2017, Caribou Creek, Canada, 19 pts
	Snow core	700	48 mm, R² = 0.92 (0.881, 32.4 mm)	Smith et al., 2017, Fortress Mountain, Canada, 8 pts
	–	0-300	±15 mm	Campbell Scientific CS725 manual[3]
		300-600	±15%	
FMCW-Radar 24 GHz	Manual snowpit	500	38 mm (14%), R² = 0.73 (0.80, 65.0 mm)	This study (Fig. 3 and 4) and Pomerleau et al., 2020, 46 pts, dry snow
	Manual snowpit	750	59 mm (30%), R² = 0.87 (0.98, 0)	Pomerleau et al., 2020, manual measurements, multi sites Northern Québec, Canada, 78 points dry snow
GNSSr	Manual snowpit	500	32 mm (11%), R²=0.93 (1.05, -7.9 mm)	This study (Fig. 4), 18 points
	Manual snowpit	2000	± 15 mm	SnowSense Vista Inc. manual[4], good conditions
	Manual snowpit	700	23 mm, R² = 0.995 (0.98, 5.52 mm)	Henkel et al. 2018, Weissfluhjoch, Switzerland (CH)
	Snow-pillow	700	11 mm, R² = 0.999 (1.01, 1.97 mm)	
	Combined data	800	66 mm, R² = 0.99 (1.1, -26 mm)	Steiner et al., 2018, Weissfluhjoch, CH, 633 pts
	Manual snowpit	1000	45 mm, R² = 0.98 (0.98, 31.4 mm) / 103 mm, R² = 0.86 (0.88, 67.3 mm)	Koch et al., 2019 dry snow, Weissfluhjoch, 3 winters / Koch et al., 2019 wet snow, Weissfluhjoch, 3 winters
	Snow-pillow and snow scale	1000	30 mm, R² = 0.99 (0.97, 30.5 mm) / 72 mm, R² = 0.93 (0.92, 65.0 mm)	Koch et al., 2019 dry snow, Weissfluhjoch / Koch et al., 2019 wet snow, Weissfluhjoch

1 https://hydroinnova.com/_downloads/snowfox_v1.pdf, Hydroinnova, Albuquerque, NM
2 Hydroinnova, Albuquerque, NM; http://hydroinnova.com/snow_water.html
3 Campbell Scientific (Canada) Corporation, CS725 manual, https://s. campbellsci.com/documents/ca/manuals/cs725_man.pdf.
4 https://www.vista-geo.de/en/snowsense/

Table 3 Pro and Cons of the four systems that were considered for SWE monitoring. SM: Soil Moisture. FOV: Field-of-View. The approximate price is given (2021), subject to change according to exchange rate fluctuations.

Sensors	CRNP		GMON	FMCW-Radar 24 GHz	GNSSr
	CRNP on the ground	CRNP above the snow			
SWEmax (mm w.e.)	Up to 2000	~150-300	600 (possibly 800)	~1000	Up to 1500
Other measured parameters	-	SM	SM	Melt detection	LWC, SD (estimated)
Other sensors needed	P, T_{air}, RH	P, T_{air}, RH	-	SD	-
Typical sampling rate	Discontinuous[a]	Discontinuous[a]	Discontinuous[a]	Continuous	Not strictly continuous[b]
Footprint	~1 - 2 m²	20-40 ha (300 000 m²)	FOV 60° Typically, 50-100 m²*	FOV ±32.5° azimuth and ±12° elevation, 0.4 m²*	~1 m²
Price (US$, 2021)	Hydroinnova: 11 000 (sensor only) EDF: Not marketed (on request)[c]		16 600 (sensor only)	1 000 (radar and software[d])	8 550 (complete station[e])
Power consumption	0.02 W, 12 V DC		0.18 W, 12 V DC	Operating: 8.14 W, 15 V DC	Operating 5 W, 12 V DC
Main advantage	Very deep snowpack	Large footprint	Medium footprint	Snowpack microstructure Very light and compact Low cost	Light SD and LWC Low cost (license only)
Main inconvenience	SM issue Needs ancillary measurements	SM knowledge needed, Needs ancillary measures Shallow snowpack	SM knowledge needed	Dry snow only	Large sky view factor required
Other drawbacks	EDF system not commercially available	Need further validation	Cost	Not turnkey Issue with ice crust	SWE for wet snow must be improved Retrieval algo. issue
Main applications, Capability (see text) Comments	Hydrology Network operational by EDF[c]	Hydrology, SM	Hydrology, SM Network operational by Hydro-Québec	SM, Stratigraphy, Avalanche, Melting monitoring Lake ice thickness RPA capability[f]	Hydrology, SM Avalanche, Melt monitoring

a: Counts must be accumulated over a specified period, e.g. 6h, 12h, or longer. b: GNSS signals must be averaged over a period of time for noise reduction; the typical measurement cycle: 1 per day (possibly up to 6 per day). c: System based on a sensor that is not commercialized. d: Software for sensor settings and reading/recording data, but not for SWE retrievals. e: Subscription license required. f: Remotely Piloted Aircraft capability.

* Depending on the height of the sensor on its support mast above snow, Field-of-View (FOV) given for 3 m mast.

Appendix

Estimating the uncertainty of in situ field measurements

In situ field measurements of Water equivalent of snow cover (SWE) are accompanied by uncertainties from a variety of sources, which include: 1) instrumental: size and type of sampling tube according to snow depth, weight scale; 2) sampling technique, extracting the snow core; 3) error that is induced by observer; 4) snow conditions: local natural variability, ice lenses and hard snow crusts within the snowpack; 5) soil conditions: irregular soil surface, identification of snow-ground interface. Snow depth is sometimes difficult to estimate over a thawed organic snow-ground interface because surface organic material is often taken into account in the snowpack depth estimate using a snow height probe.

In general, the uncertainty in the SWE depends mainly upon the diameter of the snow core according to the snow depth (the deeper the snow, the smaller the snow core that is required). Few studies discuss the accuracy of in-situ SWE measurements comprehensively over a large range of conditions, from 100 to more than 2 000 mm w.e. For example, the standard protocol that is implemented by Environment and Climate Change Canada is to attain five to ten measurements along a pre-determined survey line of about 150 to 300 m using a translucent plastic ESC-30 sampler (6.2 cm Ø, which is commonly employed in Canada) (Brown et al., 2019). Each study is generally focused on one type of snowpack. Commonly, relative uncertainty varies from 6% for shallow snowpack (0-300 mm w.e.) to 8% (300 – 1000 mm w.e.) for medium snowpack to 10-12 % for deeper snowpack (> 1000 mm w.e.) (see references in the recent review by López-Moreno et al., 2020; also see Work et al., 1965; Turcan and Loijens, 1975; Peterson and Brown, 1975; Goodison et al., 1981 and 1987; Sturm et al., 2010; Berezovskaya and Kane, 2007; Dixon and Boon, 2012; Stuefer et al., 2013; Steiner et al., 2018; Gugerli et al., 2019; Brown et al., 2019). Among recent studies, Stuefer et al. (2013) and López-Moreno et al. (2020) are limited to shallow Arctic snowpack, Steiner et al. (2018) to medium snowpack (up to 1200 mm w.e.), while Gugerli et al. (2019) discuss the problem across a large SWE range of alpine snowpacks over a glacier from 200 to 2300 mm w.e., but with the same snow core (Fig. A1).

In summary, it is well known that SWE uncertainty decreases for shallow snowpack with a larger snow core diameter (typically above 6 cm diameter), given that a larger volume of snow is sampled, Yet, on the other hand, the coring technique is more difficult when snow depth increases. For thicker snowpack, it requires the digging of a pit, because a larger core diameter impeded the retrieval of the snow sample directly from the top of the snow surface. Thus, a large snow corer is limited to shallow snowpacks (snow depth less than 1.5 – 2 m). Moreover, commonly remarks from both our experience and the above cited studies agree in that uncertainties in SWE estimates increase with thicker snowpacks. A small diameter snow core is required for thick snowpacks (snow depth above 2 m).

Figure A2 illustrates the underestimation of SWE with a large diameter snow corer when SWE increases, from a large dataset that was derived from our International Polar Year experiments (Langlois et al., 2010).
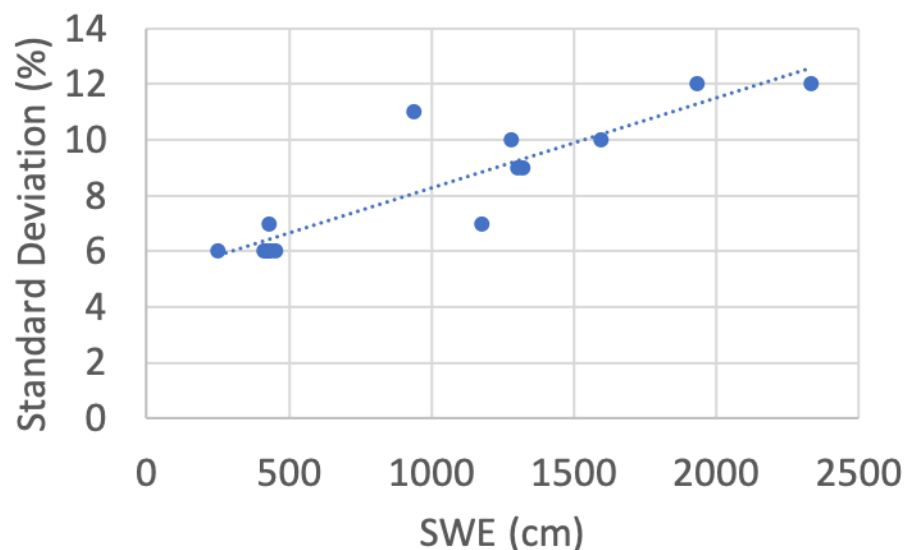
Figure A1 Relationship between the standard deviation (%) of SWE measurements as a function of SWE (mm) based on snow core, derived from Gugerli et al. (2019) (data from Glacier de la Plaine Morte, Switzerland,). Results show an uncertainty of 6 % for SWE of the order of 250 – 500 mm, about 10% for SWE between 1000 and 1500 mm, and 12% for SWE between 2000 – 2500 mm.
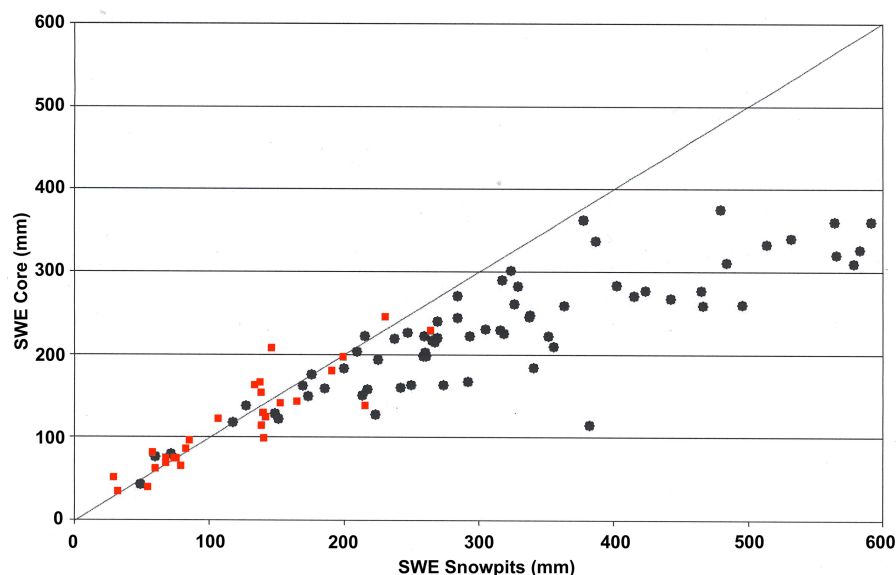

Figure A2. Comparison between SWE measurements (in mm) from snow core and snowpit methods. Red squares are for small diameter snow core (ESC-30 type core: 6.2 cm) and black points are for large diameter snow cores (9.5 cm). The black line is Y=X. Measured SWE Core values are clearly underestimated above 250-300 mm SWE. Unfortunately, no measurements with small diameter snow cores above 280 mm SWE are present in this example. The database (94 points) is derived from the International Polar Year project (Langlois et al., 2010), including sampling sites at Sherbrooke (SIRENE, 45.37° N; -71.92° W), Sept-Iles (50.30° N; -66.28° W), Schefferville (54.90° N; -66.70° W) and Kuujjuaq (58.06° N; -71.95° W) (also see Royer et al., 2021).

References

For references related to a sensor, the name of the sensor has been highlighted in **bold**.

Alonso, R., Pozo, J.M.G.d., Buisán, S.T., and Álvarez, J.A: Analysis of the Snow Water Equivalent at the AEMet-Formigal Field Laboratory (Spanish Pyrenees) during the 2019/2020 winter season using a Stepped-Frequency Continuous Wave Radar (SFCW), Remote Sens., 13, 616. https://doi.org/10.3390/rs13040616, 2021. (**SFCW radar**)

Andreasen, M., Jensen, K. H., Desilets, D., Franz, T., Zreda, M., Bogena, H., and Looms, M.C.: Status and perspectives of the cosmic-ray neutron method for soil moisture estimation and other environmental science applications. Vadose Zone J., 16, 1–11. doi: 10.2136/vzj2017.04.0086, 2017. (**CRNP**)

Appel, F., Koch, F., Rösel, A., Klug, P., Henkel, P., Lamm, M., Mauser, W., and Bach, H.: Advances in Snow Hydrology Using a Combined Approach of GNSS In Situ Stations, Hydrological Modelling and Earth Observation—A Case Study in Canada. *Geosciences*, *9*, 44. https://doi.org/10.3390/geosciences9010044, 2019. (**GNSSr**)

Berezovskaya, S. and Kane, D. L.: Strategies for measuring snow water equivalent for hydrological applications: Part 1, accuracy of measurements. Proceedings of 16th Northern Research Basin Symposium, Petrozavodsk, Russia, 22–35, 2007. (**Snow core**)

Bissell, V.C., and Peck, E.L.: Monitoring snow water equivalent by using natural soil radioactivity. Water Resour. Res., 9, 885–890, 1973. (**GMON**)

Bogena, H.R., Herrmann, F., Jakobi, J., Brogi, C., Ilias, A., Huisman, J.A., Panagopoulos, A., and Pisinaras, V.: Monitoring of Snowpack Dynamics with Cosmic-Ray Neutron Probes: A Comparison of Four Conversion Methods. Front. Water, 2, 19, doi: 10.3389/frwa.2020.00019, 2020. (**CRNP**)

Bormann, K.J., Westra, S., Evans, J.P., and McCabe, M.F: Spatial and temporal variability in seasonal snow density, J. Hydrol., 484, 63–73, 2013. (**Snow core**)

Brown, R.D., Fang, B, and Mudryk, L.: Update of Canadian Historical Snow Survey Data and Analysis of Snow Water Equivalent Trends, 1967–2016, Atmosphere-Ocean, DOI: 10.1080/07055900.2019.1598843, 2019. (**Snow core**)

Brown, R.D., Smith, C., Derksen, C., and Mudryk, L. : Canadian In Situ Snow Cover Trends for 1955–2017 Including an Assessment of the Impact of Automation, Atmosphere- Ocean, DOI: 10.1080/07055900.2021.1911781, 2021.

Carroll, T. R.: Airborne Gamma Radiation Snow Survey Program: A user's guide, Version 5.0. National Operational Hydrologic Remote Sensing Center (NOHRSC), Chanhassen, 14, https://www.nohrsc.noaa.gov/snowsurvey/, 2001. (**GMON**)

Choquette, Y., Ducharme, P., and Rogoza, J.: CS725, an accurate sensor for the snow water equivalent and soil moisture measurements, in: Proceedings of the International Snow Science Workshop, Grenoble, France, 7–11 October 2013, 2013 (**GMON**)

Clark, M. P., Hendrikx, J., Slater, A. G., Kavetski, D., Anderson, B., Cullen, N. J., Kerr, T., Hreinsson, E. Ö., and Woods, R. A.: Representing spatial variability of snow water equivalent in hydrologic and land-surface models: A review, Water Resour. Res., 47, W07539, doi:10.1029/2011WR010745, 2011.

Delunel, R., Bourles, D. L., van der Beek, P. A., Schlunegger, F., Leya, I., Masarik, J. and Paquet, E.: Snow shielding factors for cosmogenic nuclide dating inferred from long-term neutron detector monitoring, Quat. Geochronol., 24, 16–26, doi:10.1016/j.quageo.2014.07.003, 2014. (**CRNP**)

Desilets, D., and Zreda, M.: Footprint diameter for a cosmic-ray soil moisture probe: Theory and Monte Carlo simulations, Water Resour. Res., 49, 3566–3575, 2013. (**CRNP**)

Desilets, D., Zreda, M., and Ferré, T.P.A.: Nature's neutron probe: Land surface hydrology at an elusive scale with cosmic rays, Water Resour. Res., 46, 1–7, 2010. (**CRNP**)

Desilets, D.: Calibrating a non-invasive cosmic ray soil moisture probe for snow water equivalent, Hydroinnova Technical Document 17-01, doi:10.5281/zenodo.439105, 2017. (**CRNP**)

Dixon, D., and Boon, S.: Comparison of the SnowHydro snow sampler with existing snow tube designs. Hydrologic. Processes, 20, 2555-2562, DOI: 10.1002/hyp.9317, 2012. (**Snow core**)

Dong, C.: Remote sensing, hydrological modeling and in situ observations in snow cover research: A review. J. Hydrol., 561 (2018) 573–583, 2018.

Ducharme, P., Houdayer, A., Choquette, Y., Kapfer, B., and Martin, J. P.: Numerical Simulation of Terrestrial Radiation over A Snow Cover. J. Atmos. Ocean. Technol., 32, 1478-1485, 2015. (**GMON**)

Ellerbruch, D., and Boyne, H.: Snow Stratigraphy and Water Equivalence Measured with an Active Microwave System. J. Glaciol. 26, 225–233, 1980. (**FMCW-Radar**)

Evans, J. G., Ward, H. C., Blake, J. R., Hewitt, E. J., Morrison, R., Fry, M., Ball, L. A., Doughty, L. C., Libre, J. W., Hitt, O. E., Rylett, D., Ellis, R. J., Warwick, A. C., Brooks., M., Parkes, M. A., Wright, G. M. H., Singer, A. C., Boorman, D. B., and Jenkins, A.: Soil water content in southern England derived from a cosmic-ray soil moisture observing system - COSMOS-UK. Hydrological Processes, 30(26), 4987–4999. https://doi.org/10.1002/hyp.10929, 2016.

Fujino, K., Wakahama, G., Suzuki, M., Matsumoto, T., and Kuroiwa, D.: Snow stratigraphy measured by an active microwave sensor. Ann. Glaciol., 6, 207–210, 1985. (**FMCW-Radar**)

GCOS-WMO: The global observing system for climate: implementation needs, World Meteorological Organization, Geneva, Switzerland, 2016. https://public.wmo.int/en/programmes/global-climate-observing-system

Goodison, B., Ferguson, H., and McKay, G.: Measurement and data analysis, in handbook of snow: principles, processes, management, and use, Pergamon press Canada, Toronto, Canada, 191-274, 1981. (**Snow core**)

Goodison, B.E., Glynn, J.E., Harvey, K.D., and Slater, J.E.: Snow Surveying in Canada: A Perspective, Can. Water Resour. J., 12:2, 27-42, DOI: 10.4296/ cwrj1202027, 1987. (**Snow core**)

Gottardi, F., Carrier, P., Paquet, E., Laval, M.-T., Gailhard, J., and Garçon, R.: Le NRC: Une décennie de mesures de l'équivalent en eau du manteau neigeux dans les massifs montagneux français. In Proceedings of the International Snow Science Workshop Grenoble, 7–11 October 2013, 926–930, 2013. (**CRNP**)

Gray, D. M., Granger, R. J., and Dyck, G. E.: Over winter soil moisture changes, Transactions of ASAE, 28, 442–447, 1985.

Gray, D. M., Toth, B., Zhao, L., Pomeroy, J. W., and Granger, R. J.: Estimating areal snowmelt infiltration into frozen soils, Hydrol. Process., 15, 3095–3111, 2001.

GPRI brochure: GAMMA Portable Radar Interferometer (GPRI) https://gamma-rs.ch/uploads/media/Instruments_Info/gpri2_brochure_20160708.pdf , 2021. (**Radar**)

Gugerli, R., Salzmann, N., Huss, M., and Desilets, D.: Continuous and autonomous snow water equivalent measurements by a cosmic ray sensor on an alpine glacier, The Cryosphere, 13, 3413–3434, https://doi.org/10.5194/tc-13-3413-2019, 2019. (**CRNP** and **Snow core**)

Gunn, G.E., Duguay, C.R., Brown, L.C., King, J., Atwood, D., and Kasurak, A.: Freshwater Lake Ice Thickness Derived Using Surface-based X- and Ku-band FMCW Scatterometers. Cold Reg. Sci. Technol., 120, 115–126, 2015. (**FMCW-Radar**)

Haberkorn, A. (eds): European Snow Booklet – an Inventory of Snow Measurements in Europe, 363 pp., 2019.

Henkel, P., Koch, F., Appel, F., Bach, H., Prasch, M., Schmid, L., Schweizer, J., and Mauser, W.: Snow water equivalent of dry snow derived from GNSS Carrier Phases. IEEE Trans. Geosci. Remote Sens., 56(6), 3561–3572. https://doi.org/10.1109/TGRS.2018.2802494, 2018. (**GNSSr**)

Hu, X., Ma, C., Hu, R., and Yeo, T. S.: Imaging for Small UAV-Borne FMCW SAR. Sensors, 19, 87, doi: 10.3390/s19010087, 2019. (**FMCW-Radar**)

IMST: IMST sentireTM Radar Module 24 GHz sR-1200 Series User Manual. Available online: http://www.radar-sensor.com/, 2021 (**FMCW-Radar**)

Jitnikovitch, A., Marsh, P., Walker, B., and Desilets, D.: Cosmic-ray neutron method for the continuous measurement of Arctic snow accumulation and melt, The Cryosphere Discuss. [preprint], https://doi.org/10.5194/tc-2021-124, in review, 2021. (**CRNP**)

Key, J., Goodison, B., Schöner, W., Godøy, Ø., Ondráš, M., and Snorrason, Á.: A Global Cryosphere Watch. Arctic, 68, 1, 48 – 58 . http://dx.doi.org/10.14430/arctic4476, 2015.

Key, J., Schöner, W., Fierz, C., Citterio, M., and Ondráš, M.: Global Cryosphere Watch (GCW) implementation plan, World Meteorological Organization, Geneva, Switzerland, https://globalcryospherewatch.org/reference/documents/files/GCW_IP_v1.7.pdf, 2016.

Kinar, N. J., and Pomeroy, J. W.: Measurement of the physical properties of the snowpack. Rev. Geophys. 53, 481–544. doi: 10.1002/2015RG000481, 2015.

King J., Kelly, R., Kasurak, A., Duguay, C., Gunn, G., Rutter, N., Watts, T., and Derksen C.: Spatio-temporal influence of tundra snow properties on Ku-band (17.2 GHz) backscatter. J. Glaciol., 61(226), doi: 10.3189/2015JoG14J020, 2015. (**Radar**)

Kirkham, J.D., Koch, I., Saloranta, T.M., Litt, M., Stigter, E.E., Møen, K., Thapa, A., Melvold, K., and Immerzeel, W.W.: Near Real-Time Measurement of Snow Water Equivalent in the Nepal Himalayas. Front. Earth Sci. 7:177. doi: 10.3389/feart.2019.00177, 2019. (**GMON**)

Koch, F., Henkel, P., Appel, F., Schmid, L., Bach, H., Lamm, M., Prasch, M., Jürg Schweizer, J., and Mauser, W.: Retrieval of snow water equivalent, liquid water content, and snow height of dry and wet snow by combining GPS signal

attenuation and time delay. Water Resour. Res., 55, 4465–4487. https://doi.org/10.1029/ 2018WR024431, 2019. (**GNSSr**)

Koh, G., Yankielun, N.E., and Baptista, A.I.: Snow cover characterization using multiband FMCW radars. Hydrol. Process., 10, 1609–1617, 1996. (**FMCW-Radar**)

Kramer, D., Langlois, A., Royer, A., Madore, J.-B., King, J., McLennan, D. and Boisvert-Vigneault, É.: Assessment of Arctic snow stratigraphy and water equivalent using a portable Frequency Modulated Continuous Wave RADAR. Submitted to Cold Regions Science and Technology, ID.: CRST-D-21-00297, (2021).

Laliberté, J., Langlois, A., Royer, A., Madore, J.-B., and Gauthier, F.: Retrieving high contrasted interfaces in dry snow using a frequency modulated continuous wave (FMCW) Ka-band radar: a context for dry snow stability, Physical Geography, In revision (TPHY-S-21-00044), 2021. (**FMCW-Radar**) To be updated

Langlois, A., Royer, A. and Goïta, K.: Analysis of simulated and spaceborne passive microwave brightness temperature using in situ measurements of snow and vegetation properties. Can J Remote Sens. 36(S1), 135–148. doi:10.5589/m10-016, 2010.

Langlois, A.: Applications of the PR Series Radiometers for Cryospheric and Soil Moisture Research. Publisher: Radiometrics Corporation https://www.researchgate.net/publication/299372180_Applications_of_the_PR_Series_Radiometers_for_Cryospheric_and_Soil_Moisture_Research, 2015. (**Radiometer**)

Larson, K. M., and Small, E. E.: Normalized microwave reflection index: A vegetation measurement derived from GPS networks, IEEE J. Sel. Topics Appl. Earth Observ. Remote Sens., 7(5), 1501-1511, doi: 10.1109/JSTARS.2014.2300116, 2014. (**GNSSr**)

Larson, K. M.: GPS interferometric reflectometry: Applications to surface soil moisture, snow depth, and vegetation water content in the western United States. Wiley Interdisciplinary Reviews: Water, 3(6), 775–787. https://doi.org/10.1002/wat2.1167, 2016. (**GNSSr**)

Larson, K., Gutmann, E., Zavorotny, V., Braun, J., Williams, M., and Nievinski, F.: Can we measure snow depth with GPS receivers? Geophys. Res. Lett., 36, L17502. https://doi.org/10.1029/2009GL039430, 2009. (**GNSSr**)

Larue, F., Royer, A., De Sève, D., Roy, A., Picard, G., Vionnet, V.: Simulation and assimilation of passive microwave data using a snowpack model coupled to a calibrated radiative transfer model over North-Eastern Canada, Water Resour. Res., 54, 4823–4848, https://doi. org/10.1029/2017WR022132, 2018.

Leinss, S., Wiesmann, A., Lemmetyinen, J., and Hajnsek, I.: Snow Water Equivalent of Dry Snow Measured by Differential Interferometry. IEEE J. Sel. Topics Appl. Earth Observ. Remote Sens., 8(8), 3773-379, 2015. (**SnowScat radar**)

Lejeune, Y., Dumont, M., Panel, J.-M., Lafaysse, M., Lapalus, P., Le Gac, E., Lesaffre, B., and Morin, S.: 57 years (1960–2017) of snow and meteorological observations from a mid-altitude mountain site (Col de Porte, France, 1325 m of altitude), Earth Syst. Sci. Data, 11, 71–88, https://doi.org/10.5194/essd-11-71-2019, 2019.

López-Moreno, J.I., Leppänen, L., Luks, B., Holko, L., Picard, G., Sanmiguel-Vallelado, A., Alonso-González, E., Finger, D.C., Arslan, A.N., Gillemot, K., Sensoy, A., Sorman, A., Ertaş, M. C., Fassnacht, S.R., Fierz, C., and Marty, C.: Intercomparison of measurements of bulk snow density and water equivalent of snow cover with snow core samplers: Instrumental bias and variability induced by observers. Hydrol. Proc., 34, 3120-3133, https://doi.org/10.1002/hyp.13785, 2020. (**Snow core**)

Marshall, H.-P., and Koh, G.: FMCW radars for snow research. Cold Reg. Sci. Technol., 52, 118–131, 2008.

Marshall, H.-P., Schneebeli, M., and Koh, G. Snow stratigraphy measurements with high-frequency FMCW radar: Comparison with snow micro-penetrometer. Cold Reg. Sci. Technol., 47, 108–117, 2007. (**FMCW-Radar**)

Marshall, H.-P., Koh, G., and Forster, R.: Estimating alpine snowpack properties using FMCW radar. Ann. Glaciol., 40, 157–162, 2005. (**FMCW-Radar**)

Martin, J.-P., Houdayer, A. , Lebel, C., Choquette, Y., Lavigne, P., and Ducharme, P.: An unattended gamma monitor for the determination of snow water equivalent (SWE) using the natural ground gamma radiation. 2008 IEEE Nuclear Science Symposium and Medical Conference, P. Sellin, Ed., IEEE, 983–988, 2008. (**CRNP**)

Matzler, C.: Microwave permittivity of dry snow, IEEE Trans. Geosci. Remote Sens., 34, 573–581, https://doi.org/10.1109/36.485133, 1996.

Meloche, J., Langlois, A., Rutter, N., Royer, A., King, J., and Walker, B.: Characterizing Tundra snow sub-pixel variability to improve brightness temperature estimation in satellite SWE retrievals, The Cryosphere Discussion (Submitted tc-2021-156), 2021. To be updated

Meredith, M., Sommerkorn, M., Cassotta, S., Derksen, C., Ekaykin, A., Hollowed, A., Kofinas, G., Mackintosh, A., Melbourne-Thomas, J., Muelbert, M.M.C., Ottersen, G., Pritchard, H., Schuur, E.A.G.: Polar Regions. In: IPCC Special Report on the Ocean and Cryosphere in a Changing Climate [H.-O. Pörtner, D.C. Roberts, V. Masson-Delmotte, P. Zhai, M. Tignor, E. Poloczanska, K. Mintenbeck, A. Alegría, M. Nicolai, A. Okem, J. Petzold, B. Rama, N.M. Weyer (eds.)]. https://www.ipcc.ch/srocc/chapter/chapter-3-2/, 2019.

Murray, R. M., and Holbert, K. E.: Nuclear Energy: An Introduction to the Concepts, Systems, and Applications of Nuclear Processes, Eighth Edition, Imprint Butterworth-Heinemann, Elsevier Inc., 624 p. https://doi.org/10.1016/C2016-0-04041-X, 2020. (**CRNP**)

Okorn, R., Brunnhofer, G., Platzer, T., Heilig, A., Schmid, L., Mitterer, C., Schweizer, J., and Eisen, O.: Upward-looking L-band FMCW radar for snow cover monitoring. Cold Reg. Sci. Technol., 103, 31–40, 2014. (**FMCW-Radar**)

Paquet, E. and Laval, M.T.: Retour d'expérience et perspectives d'exploitation des Nivomètres à Rayonnement Cosmique d'EDF / Operation feedback and prospects of EDF Cosmic-Ray Snow Sensors. La Houille Blanche 2006-2, 113-119, 2006. (**CRNP**)

Paquet, E., Laval, M., Basalaev, L. M., Belov, A., Eroshenko, E., Kartyshov, V., Struminsky, A., and Yanke, V.: An application of cosmic-ray neutron measurements to the determination of the snow-water equivalent, Proc. 30th Int. Cosm. Ray Conf., Mexico City, Mexico, 2008, 1, 761– 764, 2008. (**CRNP**)

Peng, Z., and Li, C.: Portable Microwave Radar Systems for Short-Range Localization and Life Tracking: A Review, Sensors, 19, 1136, 2019. (**FMCW-Radar**)

Peterson, N., and Brown, J.: Accuracy of snow measurements, In Proceedings of the 43rd Annual Meeting of the Western Snow Conference, Coronado, California, 1-5, 1975. (**Snow core**)

Pieraccini, M., and Miccinesi, L.: Ground-Based Radar Interferometry: A Bibliographic Review, Remote Sens., 11(9), 1029, 2019. https://doi.org/10.3390/rs11091029. (**Radar**)

Pirazzini, R., Leppänen, L., Picard, G., López-Moreno, J. I., Marty, C., Macelloni, G., Kontu, A., von Lerber, A., Tanis, C. M., Schneebeli, M., de Rosnay, P., and Arslan, A. N.: European in-situ snow measurements: practices and purposes, Sensors, 18, 2016. doi: 10.3390/s18072016, 2018.

Pomerleau, P., Royer, A., Langlois, A., Cliche, P., Courtemanche, B., Madore, J.B., Picard, G. and Lefebvre, É.: Low Cost and Compact FMCW 24 GHz Radar Applications for Snowpack and Ice Thickness Measurements, *Sensors* 20, 14, 3909. https://doi.org/10.3390/s20143909, 2020. (**FMCW-Radar**)

Prince, M., Roy, A., Royer, A., and Langlois, A.: Timing and Spatial Variability of Fall Soil Freezing in Boreal Forest and its Effect on SMAP L-band Radiometer Measurements, Remote Sens. Environ., 231, 111230, 2019.

Proksch, M., Rutter, N., Fierz, C., and Schneebeli, M.: Intercomparison of snow density measurements: Bias, precision, and vertical resolution, Cryosphere, 10, 371–384, 2016.

Rasmussen, R., Baker, B., Kochendorfer, J., Meyers, T., Landolt, S., Fischer, A. P., Black, J., Thériault, J. M., Kucera, P., Gochis, D., Smith, C., Nitu, R., Hall, M., Ikeda, K., and Gutmann, E.: How Well Are We Measuring Snow: The NOAA/FAA/NCAR Winter Precipitation Test Bed, Bull. Am. Meteorol. Soc., 93, 811–829, 2012. (**Snow core**)

Rodriguez-Morales, F., Gogineni, S., Leuschen, C.J., Paden, J.D., Li, J., Lewis, C. C., Panzer, B., Alvestegui, D. G-G., Patel, A., Byers, K., Crowe, R., Player, K., Hale, R., Arnold, E., Smith, L., Gifford, C., Braaten, D., and Panton, C.: Advanced multifrequency radar instrumentation for polar research. IEEE Trans. Geosci. Remote Sens. 52, 2824–2842, 2014. (**FMCW-Radar**)

Roy, A., Royer, A., St-Jean-Rondeau, O., Montpetit, B., Picard, G., Mavrovic, A., Marchand, N., and Langlois, A.: Microwave snow emission modeling uncertainties in boreal and subarctic environments, The Cryosphere, 10, 623-638, http://www.the-cryosphere.net/10/623/2016/ doi:10.5194/tc-10-623-2016, 2016. (**Radiometer**)

Roy, A., Toose, P., Williamson, M., Rowlandson, T., Derksen, C., Royer, A., Berg, A., Lemmetyinen, J., and Arnold, L.: Response of L-Band brightness temperatures to freeze/thaw and snow dynamics in a prairie environment from ground-based radiometer measurements, Remote Sens. Environ., 191, 67-80, 2017. (**Radiometer**)

Rutter, N., Sandells, M. J., Derksen, C., King, J., Toose, P., Wake, L., Watts, T., Essery, R., Roy, A., Royer, A., Marsh, P., Larsen, C., and Sturm, M.: Effect of snow microstructure variability on Ku-band radar snow water equivalent retrievals, The Cryosphere, 13, 3045–3059, https://doi.org/10.5194/tc-13-3045-2019, 2019.

Rutter, N., Sandells, M., Derksen, C., Toose, P., Royer, A., Montpetit, B., Lemmetyinen, J., and Pulliainen, J.: Snow stratigraphic heterogeneity within ground-based passive microwave radiometer footprints: implications for emission modeling, J. Geophys. Res. Earth Surf., 199, 550–565, https://doi.org/10.1002/2013JF003017, 2014.

Schattan, P., Baroni, G., Oswald, S. E., Schöber, J. , Fey, C., Kormann, C., Huttenlau, M., and Achleitner, S.: Continuous monitoring of snowpack dynamics in alpine terrain by aboveground neutron sensing, Water Resour. Res., 53, 3615–3634, doi: 10.1002/2016WR020234, 2017. (**CRNP**)

Schneider, M.: Automotive radar—Status and trends. In Proceedings of the German Microwave Conference, Ulm, Germany, 5–7 April 2005; pp. 144–147, 2005. (**FMCW-Radar**)

Shah, R., Xiaolan Xu, Yueh, S., Sik Chae, C., Elder, K., Starr, B., and Kim, Y.: Remote Sensing of Snow Water Equivalent Using P-Band Coherent Reflection, IEEE Geosci. Remote Sens. Lett., 14, 3, 309-313, doi: 10.1109/LGRS.2016. 2636664, 2017. (**GNSSr**)

Sigouin, M. J. P., and Si, B. C.: Calibration of a non-invasive cosmic-ray probe for wide area snow water equivalent measurement. Cryosphere, 10, 1181–1190, 2016 www.the-cryosphere.net/10/1181/2016/, 2016. (**CRNP**)

Smith, C. D., Kontu, A., Laffin, R., and Pomeroy, J. W.: An assessment of two automated snow water equivalent instruments during the WMO solid precipitation intercomparison experiment, Cryosphere, 11, 101–116. doi: 10.5194/tc-11-101-2017, 2017. (**GMON**)

Steiner, L., Meindl, M., Fierz, C., and Geiger, A.: An assessment of sub-snow GPS for quantification of snow water equivalent, The Cryosphere, 12, 3161–3175, https://doi.org/10.5194/tc-12-3161-2018, 2018. (**GNSSr**)

Steiner, L., Meindl, M., and Geiger, A.: Characteristics and limitations of GPS L1 observations from submerged antennas, J. Geodesy, 93, 267–280, https://doi.org/10.1007/s00190-018-1147-x , 2019. (**GNSSr**)

Stranden, H. B., Ree, B. L., and Møen, K. M.: Recommendations for Automatic Measurements of Snow Water Equivalent in NVE. Report of the Norwegian Water Resources and Energy Directorate, Majorstua, Oslo, Noway, 34 p., 2015. (**GMON**)

Stuefer, S., Kane, L. D., and Liston, G. E.: In situ snow water equivalent observations in the US Arctic, Hydrol. Res., 44, 21–34, https://doi.org/10.2166/nh.2012.177, 2013. (**Snow core**)

Sturm, M., Taras, B., Liston, G., Derksen, C., Jones, T., and Lea J.: Estimating snow water equivalent using snow depth data and climate classes. Journal of Hydrometeorology, 11, 1380-1394, 2010. (**Snow core**)

Tiuri, M., Sihvola, A., Nyfors, E., and Hallikainen, M.: The complex dielectric constant of snow at microwave frequencies. IEEE J. Ocean. Eng., 9, 377–382, 1984.

Turcan, J., and Loijens, J.: Accuracy of snow survey data and errors in snow sampler measurements, Proc. 32nd East. Snow. Conf., 2-11, 1975. (**Snow core**)

Vather, T., Everson, C. S., and Franz, T. E.: The applicability of the cosmic ray neutron sensor to simultaneously monitor soil water content and biomass in an Acacia mearnsii Forest. Hydrology, 7(3), 48. https://doi.org/10.3390/hydrology 7030048, 2020. (**CRNP**)

Vriend, N.M., McElwaine, J.N., Sovilla, B., Keylock, C.J., Ash, M., and Brennan, P. V.: High-resolution radar measurements of snow avalanches, Geophys. Res. Lett., 40, 727–731, 2013. (**FMCW-Radar**)

Wallbank, J.R., Cole, S.J., Moore, R.J., Anderson, S.R., Mellor, E.J.: Estimating snow water equivalent using cosmic-ray neutron sensors from the COSMOS-UK network. Hydrological Processes, 35:e14048. https://doi.org/10.1002/hyp.14048, 2021. (**CRNP**)

Werner, C., Suess, M., Wegmüller, U., Frey, O., and Wiesmann A.: The Esa Wideband Microwave Scatterometer (Wbscat): Design and Implementation, in Proc. IGARSS 2019 - IEEE International Geoscience and Remote Sensing Symposium, 8339-8342, doi: 10.1109/IGARSS.2019.8900459, 2019. (**SnowScat**)

Werner, C., Wiesmann, A., Strozzi, T., Schneebeli, M., and Mätzler, C.: The SnowScat ground-based polarimetric scatterometer: Calibration and initial measurements from Davos Switzerland, in Proc. IEEE Int. Geosci. Remote Sens. Symp. (IGARSS'10), Jul. 2010, 2363–2366, 2010. (**SnowScat**)

Wiesmann, A., Werner, C., Strozzi, T., Matzler, C., Nagler, T., Rott, H., Schneebeli, M., and Wegmüller, U.: SnowScat, X-to Ku-Band Scatterometer Development, in Proc. of ESA Living Planet Symposium, Bergen 28.6. - 2.7. https://gamma-rs.ch/uploads/media/Instruments_Info/gamma_snowscat.pdf, 2010. (**SnowScat**)

Wiesmann, A., Werner, C., Wegmüller, U., Schwank, M., and Matzler, C.: ELBARA II, L-band Radiometer for SMOS Cal/Val Purposes, https://gamma-rs.ch/uploads/media/Instruments_Info/ELBARAII_poster.pdf, 2021. (**Radiometer**)

Wigneron, J.P., Jackson, T.J., O'Neill, P., De Lannoy, G.J., de Rosnay, P., Walker, J.P., Ferrazzoli, P., Mironov, V., Bircher, S., Grant, J.P., Kurum, M., Schwank, M., Munoz-Sabater, J., Das, N., Royer, A., Al-Yaari, A., Bitar, A. Fernandez-Moran, R., Lawrence, H., Mialon, A., Parrens, M., Richaume, P., Delwart, S., and Kerr Y.: Modelling the passive microwave signature from land surfaces: A review of recent results and application to the L-Band SMOS & SMAP soil moisture retrieval algorithms, Remote Sens. Environ., 192, 238–262, 2017. (**Radiometer**)

Work, R. A., Stockwell, H. J., Freeman, T. G., and Beaumont, R. T.: Accuracy of field snow surveys, western United States, including Alaska, Cold Regions Research and Engineering Laboratory (U.S.) Technical report, 163, 49 p., https://hdl.handle.net/11681/5580. 1965.(**Snow core**)

Wright, M., Kavanaugh, K., and Labine C.: Performance Analysis of the GMON3 Snow Water Equivalency Sensor. Proceedings of The Western Snow Conference. Stateline, NV, USA, April 2011. Poster on line, https://www.campbellsci.ca/cs725, 2011 (**GMON**)

Wright, M.: CS725 Frozen Potential: The Ability to Predict Snow Water Equivalent is Essential. METEOROLOGICAL TEChnOLOGy InTERnATIOnAL, August 2013, 122-123, https://www.meteorologicaltechnologyinternational.com, 2013. (**GMON**)

Xu, X., Baldi, C., Bleser, J.-W., Lei, Y., Yueh, S., and Esteban-Fernandez, D.: Multi-Frequency Tomography Radar Observations of Snow Stratigraphy at Fraser During SnowEx, in Proceedings of the IGARSS 2018-2018 IEEE International Geoscience and Remote Sensing Symposium, Valencia, Spain, 22–27 July 2018, 2018. (**FMCW-Radar**)

Yankielun, N., Rosenthal, W., and Robert, D.: Alpine snow depth measurements from aerial FMCW radar. Cold Reg. Sci. Technol., 40, 123–134, 2004. (**FMCW-Radar**)

Yankielun, N.E., Ferrick, M.G., and Weyrick, P. B.: Development of an airborne millimeter-wave FM-CW radar for mapping river ice, Can. J. Civ. Eng., 20, 1057–1064, 1993. (**FMCW-Radar**)

Yao, H., Field, T., McConnell, C., Beaton, A., and James A.L.: Comparison of five snow water equivalent estimation methods across categories. Hydrol. Process., 32, 1894–1908, https://doi.org/10.1002/hyp.13129, 2018. (**GMON**)